microplastics

MDPI

Article

From Antioxidant Defenses to Transcriptomic Signatures: Concentration-Dependent Responses to Polystyrene Nanoplastics in Reef Fish

Manuela Piccardo [1,*], Mirko Mutalipassi [2,3,*], Lucia Pittura [3,4], Rosa Maria Sepe [5], Pasquale De Luca [6], Laurence Besseau [7], Monia Renzi [1], Stefania Gorbi [3,4], Vincent Laudet [8], Alberto Pallavicini [1,9], Paolo Sordino [10,†] and Antonio Terlizzi [1,3,†]

[1] Department of Life Sciences, University of Trieste, Via Giorgieri, 10, 34127 Trieste, Italy; mrenzi@units.it (M.R.); pallavic@units.it (A.P.); aterlizzi@units.it (A.T.)
[2] Department of Integrative Marine Ecology, Stazione Zoologica Anton Dohrn, Villa Comunale, 80121 Naples, Italy
[3] NBFC—National Biodiversity Future Center, Piazza Marina 61, 90133 Palermo, Italy; l.pittura@staff.univpm.it (L.P.); s.gorbi@staff.univpm.it (S.G.)
[4] Department of Life and Environmental Sciences, Polytechnic University of Marche, Via Brecce Bianche, 60131 Ancona, Italy
[5] Department of Biology and Evolution of Marine Organisms, Stazione Zoologica Anton Dohrn, Villa Comunale, 80121 Naples, Italy; rosamaria.sepe@szn.it
[6] Department of Research Infrastructures for Marine Biological Resources, Stazione Zoologica Anton Dohrn, Villa Comunale, 80126 Naples, Italy; pasquale.deluca@szn.it
[7] Centre National de la Recherche Scientifique, Biologie Intégrative des Organismes Marins, Observatoire Océanologique, Sorbonne Université, 66650 Banyuls-sur-Mer, France; besseau@obs-banyuls.fr
[8] Marine Eco-Evo-Devo Unit, Okinawa Institute of Science and Technology, Tancha, 1919-1 Onna, Okinawa, Japan; vincent.laudet@oist.jp
[9] Stazione Zoologica Anton Dohrn, Villa Comunale, 80126 Naples, Italy
[10] Department of Biology and Evolution of Marine Organisms, Stazione Zoologica Anton Dohrn, Sicily Marine Centre, Contrada Porticatello, 29, 98167 Messina, Italy; paolo.sordino@szn.it
* Correspondence: manuela.piccardo@units.it (M.P.); mirko.mutalipassi@szn.it (M.M.)
† These authors contributed equally to this work and share last authorship.

Abstract

Nanoplastics (NPs) pose significant risks due to their small size and ability to penetrate biological tissues. However, the molecular pathways and cellular mechanisms affected by NP exposure in marine teleosts remain poorly understood, especially in tropical reef fishes. This study examined the impact of short-term (7 days) waterborne exposure of 100 nm-carboxyl-modified polystyrene NPs on the false clownfish (*Amphiprion ocellaris*) exposed at two daily concentrations: low (20 µg/L, environmentally relevant) and high (2000 µg/L). A multidisciplinary approach, including biochemical and transcriptomic analyses, was conducted to assess toxic effects. Biochemical assays revealed limited changes in antioxidant defenses (CAT, GR, GST, TOSC). However, the Integrated Biomarker Response index (IBRv2i) suggested a compromised physiological condition, supported by transcriptomic data. Transcriptomic profiling revealed 409 significantly differentially expressed genes (DEGs) in the high-concentration and 354 DEGs in the low-concentration groups, with 120 shared DEGs mostly upregulated and indicative of a core molecular response. Collectively, the transcriptional profile of the low-concentration group resembled an early-warning, energy-reallocation strategy aimed at preserving essential sensory functions while minimizing expendable functions. The high-concentration group amplified the shared stress signature and recruited an additional 289 unique genes, resulting in pronounced enrichment of Gene Ontology terms related to

Academic Editor: Nicolas Kalogerakis

Received: 3 October 2025
Revised: 28 October 2025
Accepted: 9 January 2026
Published: 16 January 2026

"muscle contraction", "oxygen transport", "hydrogen-peroxide catabolism", and "extracellular-matrix". This study demonstrates that PS-NP exposure can alter gene expression and physiology in juvenile reef fish, even at environmentally relevant concentrations. Molecular responses varied with concentrations highlighting the role of exposure level in influencing biological systems and potential long-term impacts of NP pollution in marine environments.

Keywords: false clownfish; *Amphiprion ocellaris*; environmentally relevant concentration; plastic pollution; toxicogenomic; IBRv2i; RNA-seq; oxidative stress; multi-biomarker

1. Introduction

The plastics industry is an ever-expanding sector, with global production exceeding 400 million tons in 2022 [1]. Due primarily to inadequate waste management, up to 12 million tons (Mt) of plastic enter the oceans each year [2], exposing ecosystems worldwide to risks whose nature and extent are still not fully understood. If current production and waste management trends continue, approximately 12,000 Mt of plastic waste will accumulate in landfills or the natural environment by 2050 [3]. Plastic pollution is now recognized as a global concern with dramatic socio-economic and ecological consequences [4]. Despite its persistence in the environment, plastic undergoes chemical, physical, and biological degradation [5,6], a process that gradually reduces its size, leading to the formation of microplastics (MPs, <5 mm) and nanoplastics (NPs, <1 µm) [7]. Like MPs, NPs can be categorized as primary (manufactured at the nanoscale) or secondary (formed through degradation). Examples of primary NPs include those used in personal care products, industrial abrasives, 3D printing, paints, and pharmaceutical delivery systems [8–10].

The concentration and distribution of NPs in the environment remain poorly characterized. Ter Halle et al. [11] were the first to report the presence of polystyrene NPs (PS-NPs) in environmental samples collected from the North Atlantic Subtropical Gyre. Since then, NPs have been detected worldwide in seawater samples [12], polar and alpine snow [13,14], lake and river water [14,15], as well as in water extracts from agricultural soil [16] and beaches [16]. However, only a handful of studies have successfully quantified NP concentrations in environmental samples. Based on current knowledge, environmentally relevant NP concentrations range from 4.2 µg/L to 563 µg/L [12,15]. Furthermore, in all cases, polystyrene is among the polymers identified in the nanometric fraction of the plastic litter.

Polystyrene (PS) is one of the most widely produced polymers worldwide, accounting for 5.2% of global plastic production. Its main applications include food packaging, eyeglass frames, and building insulation [17]. Laboratory evidence indicates that PS-NPs can form from the breakdown of larger plastic items [18–21]. Once released into the environment, PS undergoes degradation processes such as ultraviolet-induced photo-oxidation, leading to the formation of oxygen-containing functional groups, including epoxy/hydroxyl, carbonyl, and carboxyl groups [22]. This makes carboxyl-modified NPs particularly relevant for studies investigating the toxicity of environmentally aged particles. For this reason, the present study focused specifically on carboxyl-modified NPs.

Over the years, PS-NPs have been widely used in ecotoxicological studies on different aquatic organisms, including fish [23]. Laboratory experiments have demonstrated the trophic transfer of PS-NPs from primary producers to fishes [24] and their localization in different tissues during embryo development [25]. NPs have been

shown to induce various adverse effects on organismal biology. In *Carassius carassius*, weight loss, changes in muscle and liver triglyceride/cholesterol ratios, and behavioral disorders have been reported [26]. In *Oryzias sinensis* and *Zacco temminckii*, exposure to PS-NPs resulted in liver histopathological alterations, increased blood serum cholesterol levels, and locomotor deficits [24]. Additionally, in zebrafish (*Danio rerio*), the most extensively studied species in NP exposure research [27], behavioral alterations, acetylcholinesterase inhibition, genotoxic effects, and upregulation of nervous system-related genes have all been documented [28].

However, research on the impact of NPs on marine fish remains limited and often yields contrasting results [29–31]. This study aimed to extend the knowledge on the impact of NPs on marine fishes by focusing on the iconic tropical fish *Amphiprion ocellaris* (Cuvier, 1830), commonly known as the false clownfish. *A. ocellaris* belongs to the clownfishes, an iconic group of coral reef fish comprising 28 species [32]. Their distribution spans the entire tropical belt of the Indo-West Pacific Ocean, with the highest species richness found in the Coral Triangle region [33]. In clownfish, the juvenile stage marks the transition from a partially pelagic to an epibenthic lifestyle [34]. We selected juvenile specimens for testing, as the early life stages of fish are particularly vulnerable to contaminants due to their small size and underdeveloped immune system [35]. Additionally, clownfish juveniles have been shown to readily ingest polyethylene microspheres (<212 μm) in laboratory exposures [36]. The choice of clownfish as a model organism was also driven by other factors, including its increasing use in studies on the ecology, evolution, adaptation, and developmental biology of reef fish [37]. Furthermore, the availability of high-quality genome assembly and annotation [38] makes it well-suited for toxicogenomic investigations.

A multidisciplinary approach combining biochemical and transcriptomic analysis was adopted in this study to evaluate the potential toxic effect of PS-NPs in false clownfish juveniles. Specifically, considering oxidation as a key mechanism in micro- and nanoplastic aquatic toxicology [39], antioxidant responses were assessed by measuring the enzymatic activity of key enzymes, catalase (CAT), glutathione S-transferase (GST), and glutathione reductase (GR), as well by means of the TOSC (Total Oxyradical Scavenger Capacity) assay, thereby providing insights into sub-lethal stress. Although a variety of molecular, biochemical, and cytogenetic biomarkers are commonly measured in laboratory studies to assess the effects of xenobiotics on biota, summarizing the results of multiple biomarkers remains a challenge for researchers and environmental specialists. To address this issue, indexes such as the "Integrated Biological Responses version 2i" (IBRv2i) have been developed [40]. As with previous versions, the IBRv2i index is calculated using the mean biomarker responses of organisms collected in an experimental group and is based on a "reference site" or "control group" to establish the normal or basal levels of the biomarkers. Developed by Mattos and co-workers as an improvement over the previous version by Sanchez [41], the IBRv2i index has the additional advantage of preserving data variability in statistical analyses. Therefore, to facilitate a comprehensive evaluation of organism health in the context of this study, the IBRv2i index was calculated.

In parallel, a transcriptome-wide analysis of gene expression was enabled by means of Next-generation sequencing (NGS) platforms. NGS, particularly RNA sequencing, offers highly sensitive tools for rapid toxicological profiling and molecular biomarker discovery [42]. Their application in environmental monitoring is increasingly relevant across multiple stages of ecological risk assessment. However, transcriptomic studies investigating the effects of PS-NPs remain limited and variable in their findings, with no consistent molecular patterns emerging to date. Notably, existing studies utilizing RNA-

seq for PS-NP exposure have primarily focused on freshwater species [43–48], leaving a gap in knowledge regarding marine organisms.

For these reasons, the objectives of this study were to: (1) evaluate the sub-lethal effects of NPs in an iconic marine fish species, considered a potential model organism for tropical fish biology and ecology; (2) investigate whether the activation of antioxidant responses can be confirmed as a key mechanism in NP toxicity; (3) assess the adequacy and sensitivity of the IBRv2 index for the overall evaluation of fish health under NP exposure; (4) perform a transcriptome-wide analysis of gene expression to provide detailed insights into molecular alterations; (5) conduct assessments under two different contamination scenarios, one environmentally relevant and one indicative of high pollution levels, to highlight potential concentration-dependent and shared responses.

2. Materials and Methods

2.1. Nanoplastics

Carboxyl-modified PS-NP beads (hereafter referred to as PS-NPs), measuring 100 nm and internally labeled with green fluorescence (ϱ = 1.05 g/mL; excitation: 441 nm, emission: 486 nm, Figure S1), were purchased from Polysciences Inc. (Eppelheim, Germany). According to the supplier, the storage buffer contains surfactants (e.g., 0.01–0.1% Tween®20 or SDS) to aid handling. Before exposure, the stock solution was vortexed for 5 min, and the appropriate volume was directly added to each glass jar to achieve experimental concentrations of 20 µg/L (3.64×10^7 particles/mL) and 2000 µg/L (3.64×10^9 particles/mL), following the procedure outlined by Auguste et al. [49]. Particle characterization was performed in Milli-Q water and testing medium (artificial seawater, ASW) by measuring the Z-average and Polydispersity Index (PdI) using dynamic light scattering (DLS, Zetasizer Nano-ZS; Malvern Instruments Ltd., Malvern, UK) at 0, 1, and 24 h, the latter corresponding to the water renewal intervals during exposure.

2.2. Animals and Experimental Design

Juveniles of *A. ocellaris* (8.83 ± 0.57 mm standard length, 27.65 ± 6.04 mg weight) were bred at the Observatoire Océanologique de Banyuls-sur-Mer (France). In a single experiment, juveniles were placed in 1 L glass jars in a water bath to maintain temperature stability (26.3 ± 0.1 °C). Gentle aeration was provided to ensure adequate oxygenation for the well-being of the fish and for the proper mixing of PS-NPs. The photoperiod was maintained at a 13/11 light/dark cycle, and nitrite (NO_2^-) levels were randomly measured daily using the JBL NO_2 Test kit (JBL, GmbH & Co. KG, Neuhofen, Germany), remaining within acceptable limits (<0.5 mg/L). Twenty-four hours before exposure, the fish were randomly distributed into the jar system for acclimatization. The daily exposure consisted of three treatments: 0.0 µg/L (control), 20 µg/L (low), and 2000 µg/L (high). These exposure concentrations were selected based on available studies on NP effects in marine fish [30,50], and the limited research on NP presence in environmental samples [51]. Consequently, 20 µg/L can be defined as an environmentally relevant concentration, whereas 2000 µg/L is indicative of a high level of pollution.

Each treatment group consisted of 6 jars, each holding 6 animals (36 animals per group) in 0.5 L of artificial seawater per jar. The juveniles were exposed to PS-NPs for seven days. Since NPs undergo dynamic processes (aggregation) that affect their concentration and interaction with organisms [52], the test medium was renewed every 24 h (80% of the volume). The fish were fed ad libitum, with dry pellets in the morning and *Artemia salina nauplii* in the evening, coinciding with plastic administration to increase the likelihood of NPs ingestion. Mortality was monitored daily, and deceased animals were

promptly removed. At the end of the experiment, the total number of surviving and deceased fish was recorded. A mortality rate of less than 13% was recorded in the treated groups, while no deaths occurred in the control group.

2.3. Quality Control

The control of unintentional airborne contamination is a pivotal issue and represents a genuine challenge for the scientific community. Evidence of this has been reported by several authors [53]; however, specifically for nanoplastics, contamination remains, to date, entirely potential and has not yet been quantified experimentally due to technological limitations [54,55]. That said, several precautions can be taken to at least limit unintentional microplastic contamination. The experiment was conducted in a dedicated, windowless chamber accessed only by the researcher responsible for the experiment, who ensured that all glassware was thoroughly washed with abundant deionized water before use, wore nitrile gloves, and dressed in cotton clothing. Furthermore, the daily replacement of 80% of the water should have further reduced the risk of accumulation of any airborne microplastic fibers in the aquaria.

2.4. Bioaccumulation

Bioaccumulation assessment is a critical component of ecotoxicological studies. To evaluate the PS-NP uptake, we exposed clownfish juveniles to internally fluorescent labeled NPs. Particle bioaccumulation was assessed using a protocol involving tissue digestion in KOH, followed by fluorescence quantification via spectrofluorimetry (6 animals per treatment). However, this method failed to yield conclusive results, as particle-specific fluorescence could not be reliably distinguished from background signals. Several factors may have contributed to this outcome, including the low exposure concentrations and potential interference from the diet provided during the experiment. Another inconclusive attempt was the histological analysis following paraffin embedding and confocal microscopy (6 animals per treatment). While this represents a limitation of the study, we are nevertheless confident that a direct NP–fish interaction occurred, as supported by the results of the biochemical and molecular analyses which highlighted not only significant differences between treated and control groups but also concentration-dependent responses. In our case, therefore, the absence of evidence of bioaccumulation can be attributed to objective technological limitations and to non-ideal, contingent choices (i.e., the autofluorescence of the food/tissues). Future studies will certainly aim to improve this aspect.

2.5. Biochemical Analysis

To evaluate biochemical responses related to antioxidant defenses, the activities of specific enzymes, including catalase (CAT), glutathione S-transferase (GST), and glutathione reductase (GR), were measured. Additionally, the Total Oxyradical Scavenging Capacity Assay (TOSCA) was employed to quantify the scavenging capacity to both peroxyl (ROO·) and hydroxyl (HO·) radicals.

At the end of the exposure, 18 juveniles (6 per concentration) were randomly selected and euthanized by immersion in a tricaine methanesulfonate (MS-222, Sigma-Aldrich, St. Louis, MO, USA, Lot.wxbc9102v) bath (200 mg/L). The entire juvenile was then homogenized in a 1:10 *w*/*v* ratio in 100 mM K-phosphate buffer (pH 7.5) containing 0.008 TIU/mL aprotinin, 1 mg/mL leupeptin, and 1.8% NaCl. The homogenate was centrifuged at 110,000× *g* for 1 h at 4 °C. Enzymatic activities were measured using a spectrophotometer at a constant temperature of 20 °C, while TOSC was quantified through a gas chromatographic assay. Standardized protocols were followed to measure biomarkers in the tissues

of both control and exposed organisms. Detailed methods are provided in the Supplementary Materials.

2.6. IBRv2i Index

To summarize and simplify the interpretation of biomarker responses, the "Integrated Biological Responses version 2i" index (IBRv2i) was utilized [40], providing an overall assessment of the organism's health status. The IBRv2i index is an improvement over the version proposed by Sanchez et al. [41], as it preserves individual data variability, allowing its use for statistical tests. It is based on the concept of a "control group" reference deviation to establish the normal or basal levels of the biomarkers. The magnitude of the index values can be interpreted as the impact of PS-NPs on organisms: higher index values indicate poorer health status or more stressed organisms.

To compare the biomarker responses between tested and control organisms, we additionally calculated Cliff's delta [56] as suggested by Pham et al. [57]. The use of Cliff's delta offers several advantages: insensitivity to violations of normality and homoscedasticity, unequal sample sizes, and extreme values, as well as the ability to use both ordinal and continuous data [57]. More specifically, for a biomarker X measured in n_c individuals from the control group (denoted as x_c) and n_t individuals from the test group (denoted as x_t), Cliff's delta is calculated as follows:

$$d = \frac{\#(x_t > x_c) - \#(x_t < x_c)}{(n_t \times n_c)} \quad (1)$$

where # denotes the number of replicates. Cliff's delta measures the non-overlap between the distribution of responses in the test group and the distribution of responses in the control group. It ranges from −1 (where all responses in the test group are lower than those in the control) to 1 (where all responses in the test group are higher than those in the control). A Cliff's delta of zero indicates that the two distributions fully overlap. Cliff's delta results, represented as a heatmap, will enable the visual detection of biomarker activation patterns, avoiding the use of a radar chart, which is highly dependent on the ordering of biomarkers and has been criticized for this reason [57].

2.7. Molecular Analysis

2.7.1. RNA Extraction

Following the exposure, 18 juveniles (6 per treatment) were randomly selected, euthanized by thermal shock, and stored in TRIzol™ reagent (Thermo Fisher Scientific, Waltham, MA, USA) at −80 °C until further analysis. Total RNA was extracted according to the manufacturer's instructions, and the samples were resuspended in 30 µL of RNase-free water. RNA quality and concentration were determined using an Agilent 2100 Bioanalyzer System (Agilent Technologies, Santa Clara, CA, USA), a NanoDrop ND-1000 spectrophotometer (Thermo Fisher Scientific, Waltham, MA, USA), and TapeStation 4200 (Agilent Technologies, Santa Clara, CA, USA).

2.7.2. RNA-seq

For RNA-seq analysis, 4 samples per treatment were selected and sent to Genomix4life S.r.l. (Baronissi, SA, Italy). Indexed libraries were prepared from 800 ng of purified RNA using the TruSeq Stranded mRNA Sample Prep Kit (Illumina, Inc., San Diego, CA, USA), following the manufacturer's instructions. The libraries were quantified using the TapeStation 4200 and a Qubit™ fluorometer (Invitrogen, Thermo Fisher Scientific, Waltham, MA, USA).. The indexed libraries were pooled in equimolar amounts, achieving a final concentration of 2 nM. The pooled samples underwent cluster generation and sequencing on an Illumina NextSeq 550 System (Illumina) in a 2 × 75 paired-end format at a final concentration of 1.8 pmol.

To initially explore the overall biological structure of the data, a non-metric MDS plot on the Bray–Curtis matrix of untransformed data of all transcripts with TPM (Transcripts Per Million) > 1, was created with PRIMER v7 [58]. Differential gene expression analysis was conducted using the Differential Expression for RNA-Seq tool, which performs statistical testing across a set of Expression Tracks with associated metadata. This tool supports multi-factorial analysis using a negative binomial Generalized Linear Model (GLM) framework, allowing for robust modeling of biological and technical variability. Differential gene expression between the control and exposed fish was evaluated, allowing for no more than 2 mismatches per read. Genes with a false discovery rate (FDR) p-value ≤ 0.05 were considered differentially expressed (DEGs) and were subsequently defined as significantly altered when displaying a fold change (FC) greater than |1.5|. Gene Ontology (GO) enrichment analysis was performed using the Gene Set Test tool within CLC Genomics Workbench. It performs hypergeometric tests to evaluate whether GO terms are significantly overrepresented among the differentially expressed genes, compared to the full set of expressed genes.

2.8. Statistical Analyses

Biochemical data were analyzed using GraphPad Prism software v. 8.0.1 (GraphPad Software, San Diego, CA, USA). Biochemical response data were first tested for normality with the Shapiro–Wilk test and for homogeneity of variance with Bartlett's test. When the data met the assumptions of ANOVA, Dunnett's and Tukey's multiple comparison tests were applied to identify significant differences versus the control and among treatments, respectively. If the assumptions for ANOVA were not met, a non-parametric test (Kruskal–Wallis) was used instead. A p-value threshold of less than 0.05 was considered statistically significant. For the calculation of the IBRv2i index and Cliff's delta, Microsoft Excel was used.

3. Results

3.1. Nanoparticles' Behavior in Fresh and Seawater

DLS analysis revealed distinct dispersion patterns of PS-NPs in different media. In Milli-Q water, PS-NPs exhibited optimal dispersion, with Z-average values of 125.1 ± 3.5 nm (mean ± st. dev.) and a low PdI of 0.2 ± 0.1 (mean ± st. dev.). These values remained stable over time and across different concentrations, suggesting that the nanoparticles were well dispersed and stable in Milli-Q water. In contrast, when dispersed in ASW, PS-NPs exhibited significantly higher Z-average values of 1457.4 ± 573.9 nm (mean ± st. dev.) and a higher PdI of 0.6 ± 0.1 (mean ± st. dev.), indicating the formation of aggregates at the micro scale (see Supplementary Materials, Figure S2). Notably, the size of these aggregates varied over 24 h. In light of these results, which confirm a well-known dynamic behavior tending toward aggregation, the decision to renew the medium every 24 h was therefore necessary to mitigate undesirable effects on NP concentration and NP-organism interaction.

3.2. Biochemical Responses Related to Oxidative Stress and Health Status

No statistically significant differences were found in the activities of CAT, GST, GR and for the TOSC assay (Figure 1a). A concentration-dependent response was not detected, as indicated by the test comparing treatments (p-value > 0.05). However, the health status of the fish exposed to PS-NPs was found to be deteriorated compared to the control group, as indicated by the mean IBRv2i values, which were 2.53, 4.89, and 4.56 for the control, low, and high groups, respectively. Moreover, although the p-value was modest (0.0469), the low treatment was also found to be statistically different from the control (Figure 1b).

The activation patterns of biomarkers in the low and high groups are similar (Figure 1c). GR and TOSC HO˙ were either not involved at all or only marginally involved (Cliff's delta < 0.2). Negative Cliff's delta values (<−0.36) for GST indicate responses in the treated groups lower than the control. Meanwhile, the biomarkers that appear to be most activated, corresponding to higher production, are CAT and TOSC ROO˙.

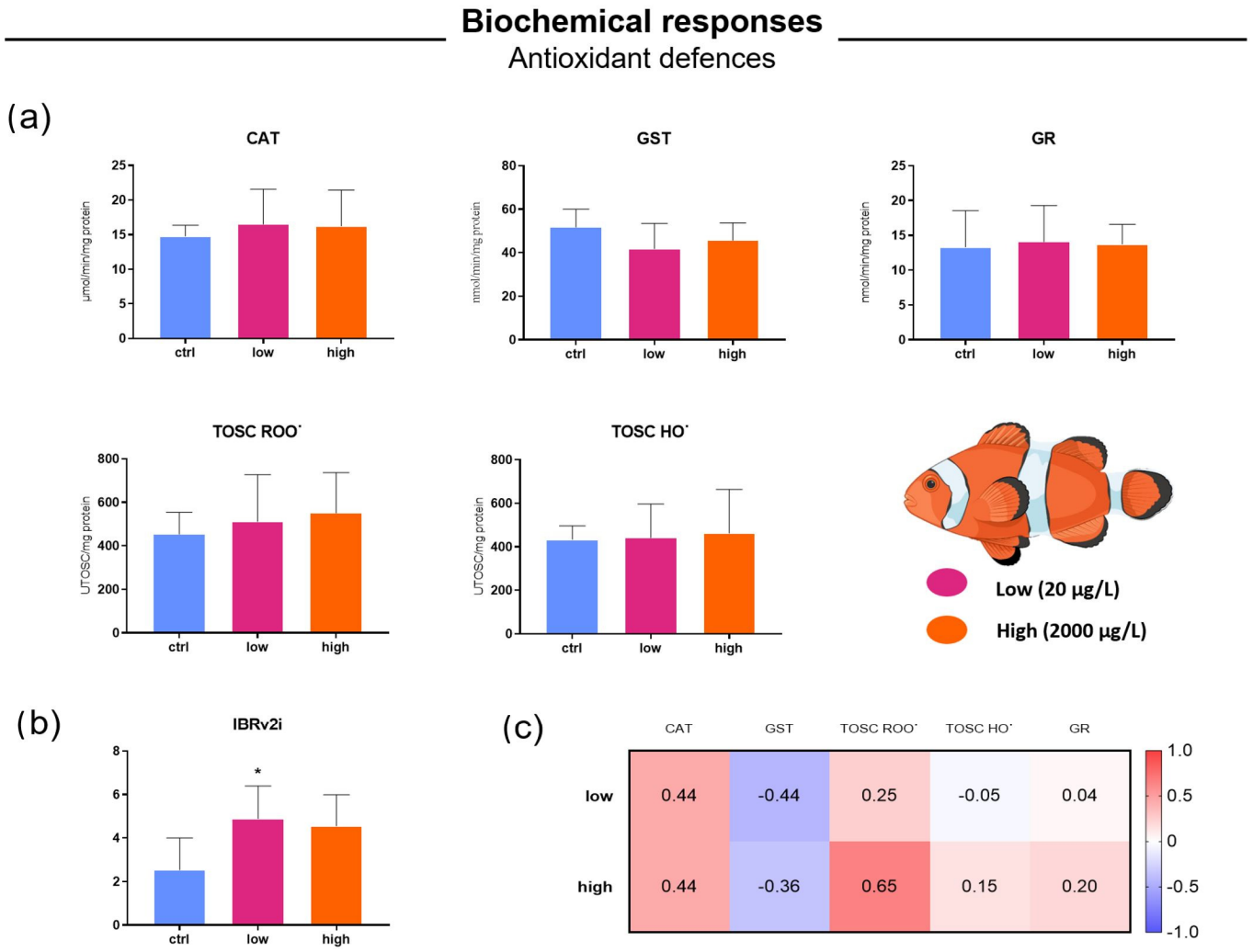

Figure 1. Antioxidant defenses in false clownfish juveniles exposed to 100 nm PS-NPs for 7 days to the daily concentrations of 20 μg/L (low) and 2000 μg/L (high). (**a**) Levels of catalase (CAT), glutathione S-transferase (GST), glutathione reductase (GR), n = 5; Total Oxyradical Scavenging Capacity toward peroxyl radical (TOSC ROO˙) and hydroxyl radical (TOSC HO˙), n = 4. (**b**) Values of the Integrated Biomarker Response version 2 Index (IBRv2i). (**c**) Heatmap with Cliff's delta computed for the six biomarkers related to oxidative stress responses. Ctrl = control group. Data are expressed as mean values ± standard deviation. * means statistically different (*p*-value < 0.05) from control group.

3.3. Transcriptomic Responses

The non-metric MDS plot revealed a clear separation of the transcriptome profile between control and treated samples (see Supplementary Materials, Figure S3). Moreover, the two treatment concentrations exhibited both divergence and overlap, suggesting the presence of shared transcriptomic responses as well as concentration-dependent differences. These distinctions became even more apparent upon analysis of the differentially expressed genes, which revealed a total of 354 DEGs in the low group (20 μg L^{-1}), 409

DEGs in the high group (2000 µg L^{-1}), and 120 DEGs shared between the two treatments. The transcriptome dataset is available on Zenodo (https://doi.org/10.5281/zenodo.17432021).

3.3.1. Shared Responses

A common set of 120 genes responded to NP exposure regardless of concentration, suggesting a core transcriptional response (Figure 2a). Many of these shared genes likely encode key components of the cellular stress response, including antioxidant enzymes, molecular chaperones, and metabolic enzymes. All shared genes were significantly altered (FC > |1.5|); specifically, 74 genes were upregulated, while 46 were consistently downregulated (Figure 2c). Moreover, to assess the magnitude and consistency of expression changes between the two conditions, we examined the $\log_2$ fold changes ($\log_2$ FC) of the 120 shared DEGs across high and low exposure levels. A direct comparison revealed a strong and statistically significant Spearman correlation (ρ_S = 0.9522, *p*-value < 0.001) between treatments: genes that were strongly induced at the high concentration also tended to be upregulated at the low concentration, albeit often to a lesser extent, and similarly for downregulated genes (Figure 2b).

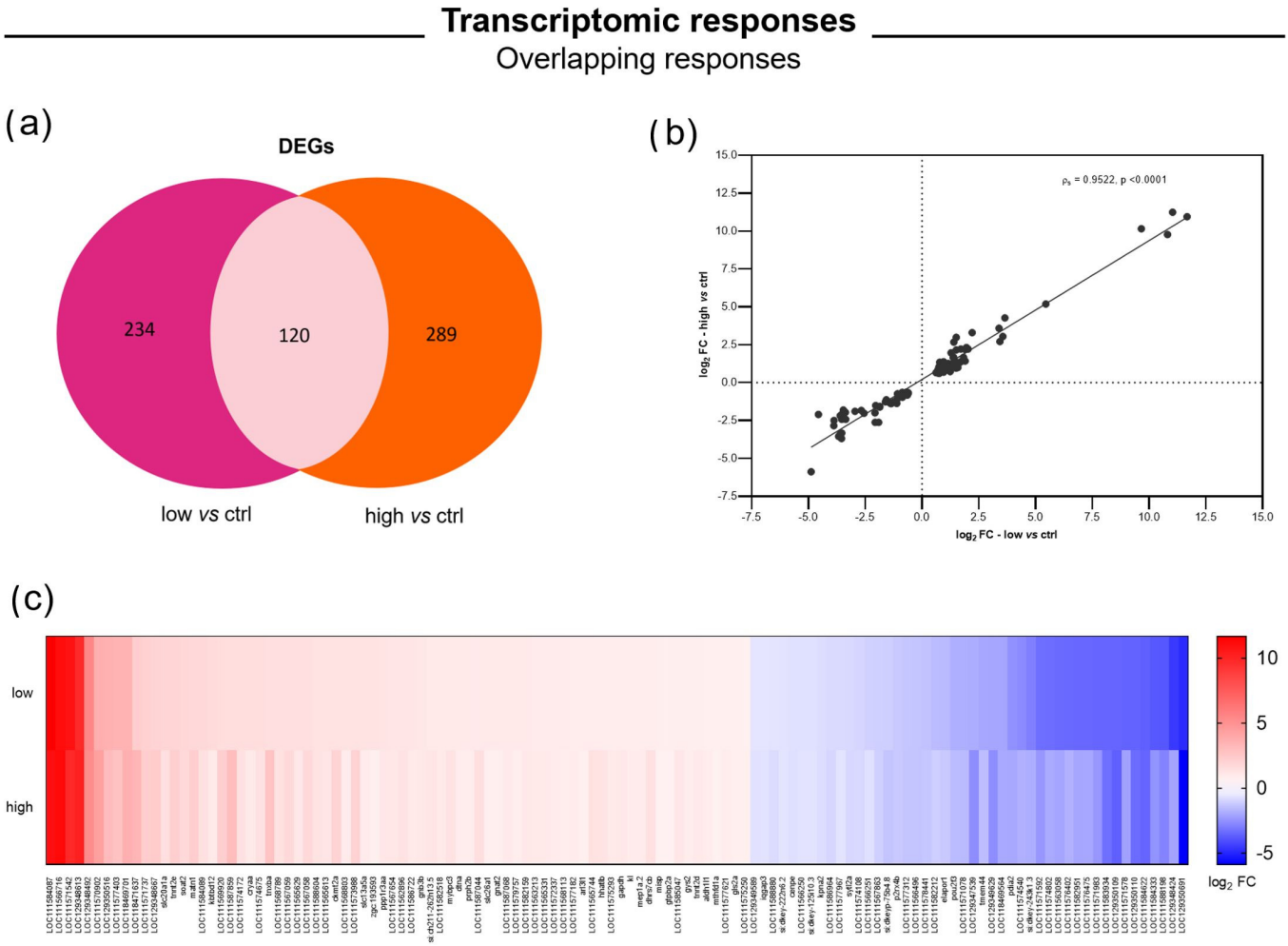

Figure 2. Shared transcriptomic responses in false clownfish juveniles exposed to 100 nm PS-NPs for 7 days to the daily concentrations of 20 µg/L (low) and 2000 µg/L (high). (**a**) Venn diagram showing DEGs in clownfish exposed to NP concentrations compared to the control group (DEGs = FDR ≤ 0.05). (**b**) Fold-change correlation for the 120 shared DEGs between high and low NP exposures. Each point represents a gene significantly dysregulated under both conditions, plotted by its $\log_2$

fold change in the high vs. control comparison (*y*-axis) and in the low vs. control comparison (*x*-axis). Points located in the second and fourth quadrants indicate genes regulated in the same direction under both treatments (all shared genes fell into these quadrants, with no gene reversing its direction of regulation between concentrations). The diagonal trend suggests that many genes exhibit similar fold-change magnitudes at both concentrations, although several genes show attenuated responses at the lower concentration (with points falling closer to either the *x*-axis or *y*-axis). (**c**) Heatmap of the 120 DEGs significantly altered in clownfish exposed to low and high NP concentrations.

3.3.2. Concentration-Dependent Responses

Despite the significant overlap, each concentration also triggered a substantial number of unique DEGs (Figure 3a). Low exposure induced 234 unique DEGs not observed under high exposure, while high exposure led to 289 genes that were not affected at the low concentration (Figure 2a). In both treatments, the majority of DEGs were upregulated: 72% at the high and 65% at the low concentration, with the latter showing a slightly higher proportion of downregulated genes (Figure 3a). To explore the biological significance of these changes, we performed a functional enrichment analysis for each condition, focusing on GO terms associated with upregulated and downregulated gene sets.

Functional Enrichment—Low Exposure

Fish exposed to the low concentration of NPs exhibited significant changes in gene expression; however, the affected functional categories differed markedly from those observed in the high group. DEGs were particularly enriched in processes related to sensory systems, especially vision, and neurodevelopment, as well as in certain metabolic and stress-related pathways (Table S1).

GO Biological Process (BP) enrichment revealed a striking emphasis on sensory and neurological functions (Figure 3b). The most significantly enriched BP terms (FDR < 0.001) included "lens development in camera-type eye" (GO:0002088), "visual perception" (GO:0007601), "sensory perception of light stimulus", and the broader category "sensory perception" (GO:0007600). These enrichments were driven by the upregulation of multiple genes involved in eye structure and function. Several crystallin genes, such as *cryaa*, *cryba1a*, and members of the *crybb1* family, which encode key structural proteins of the eye lens, were among the most strongly upregulated genes at low NP concentration. For example, *cryaa* (alpha-crystallin A) showed an approximately 2.8-fold increase at low concentration (and a modest upregulation at high concentration), while *beta-crystallins like crybb1* and *cryba4* were also upregulated by around 2-fold. These transcriptional changes explain the significant enrichment of the GO Molecular Function (MF) term "structural constituent of eye lens" (GO:0032052), which emerged as the top MF category among genes dysregulated by low-concentration exposure, with extremely strong enrichment (FDR~6.9×10^{-8}; Figure 3b; Table S1). This MF term reflects the overexpression of lens structural proteins, suggesting that pathways related to eye development or maintenance may be activated in response to low-level NP exposure. After FDR correction, no other MF categories reached statistical significance. Some nominal enrichment was observed for terms such as "sterol esterase activity" and "serine-type peptidase activity", each driven by a small number of upregulated enzymes (e.g., a retinol dehydrogenase or a serine protease), but these did not meet the FDR ≤ 0.05 threshold. Similarly, structural molecule activity had a raw *p*-value of ~7.8×10^{-5}, but its FDR (~0.12) rendered it non-significant, primarily due to overlap with crystallins and other structural proteins.

In line with the visual system theme, we also observed upregulation of retinoid-binding proteins. Notably, *RBP3* (retinol-binding protein 3, also known as interphotoreceptor retinoid-binding protein) was significantly upregulated (~2-fold) in fish exposed to the

low NP concentration. *RBP3* plays a critical role in the visual cycle by transporting retinoids (vitamin A derivatives) between photoreceptors and retinal pigment epithelial cells. Its induction may indicate activation of the retinal visual cycle or a compensatory mechanism to preserve visual function under stress. The enriched GO Biological Process term "sensory perception of light stimulus" (GO:0050953) includes such genes involved in photo-transduction and retinal processing. Additionally, the term "neurological system process" (GO:0050877) was enriched, suggesting that genes involved in neuronal function and development were also upregulated. These may include genes relevant to neuronal growth or signaling, potentially shared between sensory neurons and other neural cell types.

The GO Cellular Component (CC) results for DEGs at low NP concentration did not reveal any highly significant enrichment after correction for multiple testing. There was marginal enrichment for terms related to muscle structures, for example, contractile fiber part (GO:0044449) showed a raw *p*-value of approximately 6×10^{-5}, but an FDR of ~0.07. This suggests that a subset of muscle-related genes, possibly overlapping with those affected at high concentration, were also induced at the low concentration, albeit to a lesser extent, resulting in enrichment that did not reach statistical significance. Indeed, the low concentration did upregulate a few muscle-related genes. For instance, *tnnt2e* (a *troponin* T gene) showed modest induction and is included in the contractile fiber category. However, this muscle-related transcriptional response was notably weaker than that observed at high NP concentration. Interestingly, no significant CC terms related to eye structures, such as photoreceptor parts or synapses, were enriched. This may be due to insufficient annotation specificity or to the fact that the key genes involved (e.g., crystallins) are primarily annotated with broad terms like cytosol rather than with structure-specific CC terms.

Finally, no clear pattern of downregulated genes or biological processes emerged at the low NP concentration. However, individual gene-level analysis revealed some downregulation of metabolic genes (*pdia2*, *psmb10*) and immune-related genes (*btk*, *ccl34b*.4, as well as *psmb10*). Notably, there was a modest downregulation of certain digestive enzyme genes and genes involved in proteolysis, which may suggest a subtle suppression of digestive or metabolic activity in response to low-level exposure, potentially reflecting an energy-conserving or stress-adaptive response.

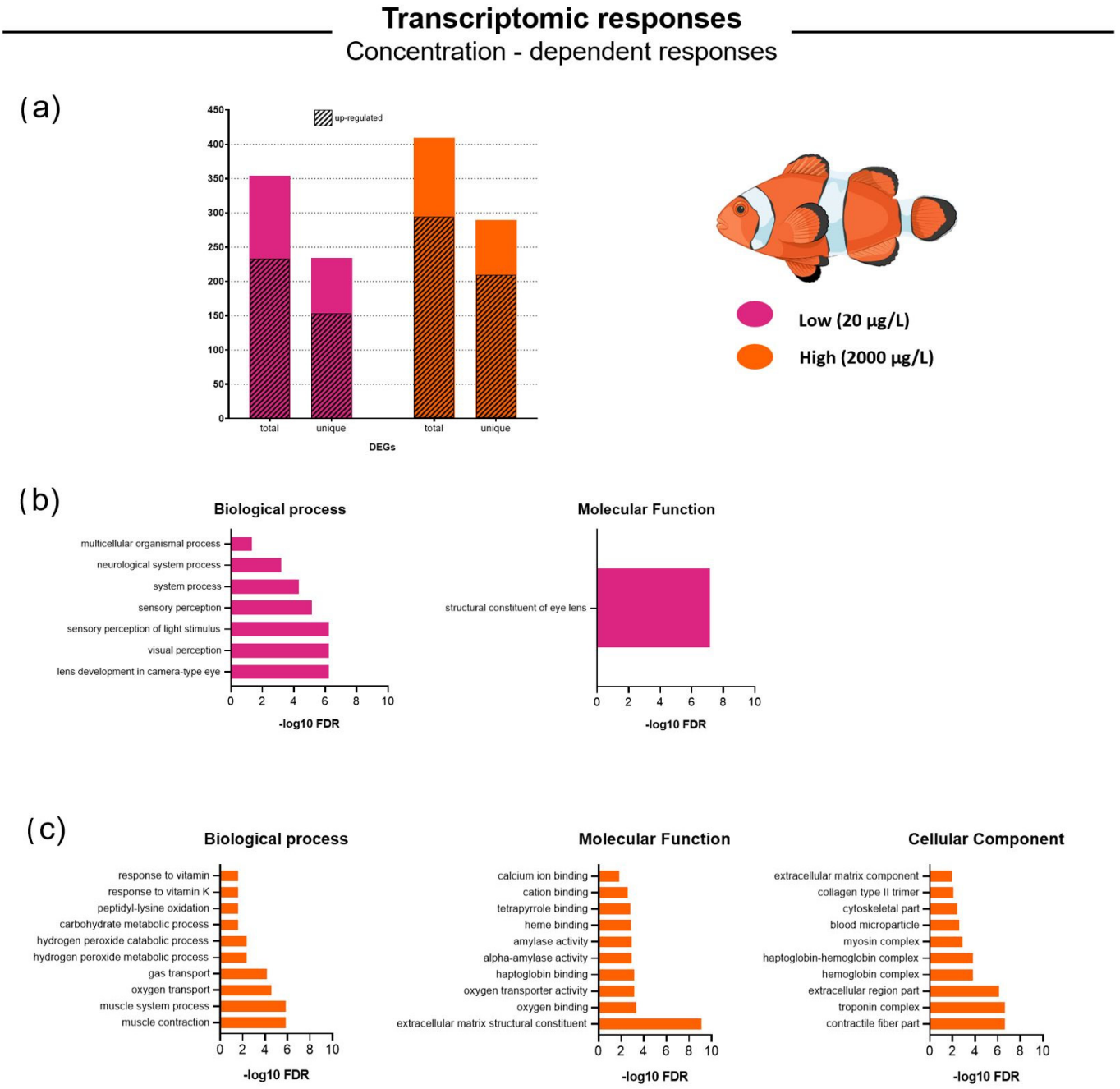

Figure 3. Concentration-specific transcriptomic responses in false clownfish juveniles exposed to 100 nm PS-NPs for 7 days to the daily concentrations of 20 µg/L (low) and 2000 µg/L (high). Gene expression analysis: (**a**) bar-plot of total and concentration-specific (unique) differentially expressed genes (DEGs, control vs. low and control vs. high). GO enrichment analysis with representation of terms ranked by significance, represented as $-\log_{10}$(FDR) on the *x*-axis: (**b**) enriched GO terms in response to low PS-NP concentration exposure (GO terms under the "Cellular Component" category are not shown, as no highly significant enrichment was observed for this category); (**c**) top 10 enriched GO terms for up-regulated genes differentially expressed in response to high PS-NP concentration exposure.

Functional Enrichment—High Exposure

GO enrichment analysis of DEGs from the high-concentration group revealed dozens of significantly enriched terms across the Biological Process, Cellular Component, and Molecular Function categories (Figure 3c). Many of the top-ranking GO terms were linked

to muscle contraction, extracellular matrix organization, and oxidative stress/antioxidant activity, suggesting that these processes represent central components of the transcriptional response to high-concentration NP exposure (Table S2).

In the Biological Process domain, the most significantly enriched terms (based on FDR) among dysregulated genes included: "muscle contraction" (GO:0006936), "muscle system process" (GO:0030012), "oxygen transport" (GO:0015671), "gas transport"(GO:0015669), "hydrogen peroxide metabolic process" (GO:0042743), and "hydrogen peroxide catabolic process" (GO:0042744), among others. Figure 3c presents the top 10 enriched BP terms for upregulated DEGs at high NP concentrations. Processes related to muscle contraction and the muscle system were among the most enriched, pointing to a coordinated dysregulation of genes involved in muscle function. Also highly enriched were "oxygen transport" and "gas transport processes", largely driven by increased expression of hemoglobin and myoglobin subunit genes (*hbae5*, *hbbe2*, *mb*, *cygb2* as well as two hemoglobin isoforms annotated as LOC111574807 and LOC111574808), which are key players in oxygen binding and delivery. The enrichment of the "hydrogen peroxide metabolic" (GO:0042743) and "catabolic processes" (GO:0042744) suggests an upregulation of antioxidant defense mechanisms, particularly enzymes involved in the breakdown of H_2O_2. Several metabolic processes were also overrepresented, including "carbohydrate metabolism" (GO:0005975) and "peptidyl-lysine oxidation" (GO:0018057), the latter playing a role in collagen cross-linking and other post-translational modifications. Terms related to vitamin response, such as "response to vitamin K" (GO:0032571) and "response to vitamin" (GO:0033273), were also enriched, suggesting possible disruptions in vitamin-dependent metabolic or signaling pathways, particularly those involving bone formation, coagulation, or other vitamin-mediated physiological functions. Overall, the enrichment of these biological processes among dysregulated genes indicates that exposure to high NP concentrations triggers a broad physiological stress response. This includes enhanced muscle and respiratory activity (potentially compensating for impaired oxygen transport), activation of antioxidant pathways to manage oxidative stress, and adjustments in energy metabolism and vitamin-related functions.

The Cellular Component GO enrichment for high-concentration dysregulated genes was dominated by muscle fiber and extracellular matrix-related terms (Figure 3c). The top CC terms for high-concentration DEGs (focusing on upregulated genes) were "contractile fiber part" (GO:0044449, which includes actin–myosin filament structures in muscle) and "troponin complex" (GO:0005861, a calcium-binding regulatory complex in muscle fibers). This, along with increased transcription of structural muscle proteins such as troponin subunits *Tnni* and *Tnnt2e*, suggests a strong enrichment of muscle fiber components, particularly troponin and myosin proteins, among the genes induced at this concentration. Other enriched terms included "extracellular region part" (GO:0044421), consistent with the overexpression of secreted proteins and components like collagens, as well as "hemoglobin complex" (GO:0005833), and "haptoglobin–hemoglobin complex" (GO:0031838), reflecting elevated expression of hemoglobin subunits and their binding proteins. Other notable enriched terms included the "myosin complex" (GO:0016459, another key component of muscle fibers), "blood microparticle" (GO:0072562, which may reflect changes in blood plasma or vesicle-related physiology), "cytoskeletal part" (GO:0044430), "collagen type II trimer" (GO:0050585), and "extracellular matrix component" (GO:0044420).

Consistent with these processes, the Molecular Function enrichment for high-concentration dysregulated genes was dominated by structural and binding activities relevant to muscle and blood (Figure 3c). The most significant MF term was "extracellular matrix structural constituent" (GO:0005201), driven by the strong induction of multiple collagen genes. This indicates enhanced production of extracellular matrix (ECM) components,

possibly as a repair or protective mechanism in response to tissue damage from NPs. Other enriched MF terms included "oxygen binding" (GO:0019825) and "oxygen transporter activity" (GO:0005344, reflecting up-regulation of hemoglobin and myoglobin genes), "heme binding" and "tetrapyrrole binding" (related to hemoproteins like hemoglobin), and enzymatic activities such as "alpha-amylase activity" (suggesting changes in digestive or metabolic enzyme expression). The MF enrichment underscores that collagens (ECM proteins) and hemoglobin (oxygen transport) were among the most up-regulated gene products in the high-concentration group. For example, collagens like *Col1a1* and *Col11a1* showed high induction (multiple collagen isoform genes had $\log_2$ FC > 3), and several hemoglobin subunits (identified as LOC111574807, LOC111574808, etc., likely globin genes) were also strongly up-regulated. The ECM up-regulation is notable – it points to potential fibrosis or wound-healing-like processes, which could be a reaction to NPs-induced tissue injury or inflammation in organs like gills or gut.

Fewer GO terms were significantly enriched among down-regulated DEGs, consistent with the smaller number of repressed genes. There was no single dominant functional theme among the down-regulated genes akin to the up-regulated patterns. However, some down-regulated genes at high concentration included those involved in sensory or developmental pathways that might have been constitutively expressed in controls and became suppressed under severe stress, as in the case of *p2rx4b*, *ltb4r2a/b*, *ildr1a* (respectively, chemosensory purinergic receptor, leukotriene-B4 receptors, inner-ear cadherin). For instance, we observed that certain neuronal or signaling genes (e.g., a subset of genes associated with developmental signaling, as in the case of Wnt-receptor-like LOC111574971 and Hedgehog-like LOC111574108) were down-regulated at high concentration. However, these did not enrich significant GO categories above the threshold. High NP load may divert the organism's resources away from growth and development-related gene programs, leading to their suppression. The net effect, however, appears to be dominated by active up-regulation of protective and compensatory mechanisms rather than broad gene suppression.

4. Discussion

Plastic litter has been documented across all marine and coastal ecosystems, including some of the most remote and biodiverse regions [15,59–61]. Among these, tropical reef systems, already under pressure from natural disturbances and anthropogenic stressors [62], are increasingly affected by plastic pollution. While microplastics have been identified in tropical reef fishes [63,64], the physiological and molecular effects of nanoplastics remain largely unexplored [65]. In this study, juvenile clownfish (*Amphiprion ocellaris*) were exposed to 100 nm carboxyl-modified polystyrene nanoplastics for seven days to investigate sub-lethal biochemical and transcriptomic responses.

4.1. Biochemical Analysis: Slight or Negligible Activations of Oxidative Stress Responses

Oxidative stress resulting from the excessive production of reactive oxygen species (ROS) has been recognized as a key mechanism in micro- and nanoplastic aquatic toxicology [39]. The elevated ROS load necessitates adaptive responses in animals, involving detoxifying enzymes and low molecular weight scavengers. Fish appear to possess similar biochemical pathways of mammalian species to cope with the toxic effects of both endogenous and exogenous agents [66]. In this experiment, the activity of sensitive biomarkers such as CAT, GST, and GR in clownfish juveniles exposed to NPs did not show statistically significant differences. These findings are consistent with those reported in other studies. Chen et al. [28] tested the toxicity of NPs in zebrafish larvae (50 nm; 1000 μg/L), revealing CAT and GPx levels comparable to those of control animals. Pitt et al. [67] examined the effects of 42 nm PS-NPs (at 10% of food by mass) in male and female zebrafish,

reporting no statistically significant differences in CAT activity. Moreover, CAT levels in the gut of female mosquitofish exposed to 700 µg/L of PS-NPs (80 nm) were not affected after 96 h of exposure [68]. Conversely, oxidative stress has been observed in adult zebrafish but only after a chronic exposure (28 days) to 500 µg/L of 100 nm PS-NPs (decreased levels of catalase and glutathione [43]), and in *Sparus aurata* specimens exposed to higher NP concentrations (10 mg/L) for a shorter period (24–96 h). Here, antioxidant-related genes (e.g., *gpx1*, *sod2*, *gr*) were upregulated [30]. Discrepancies between studies may be due to several factors, including differences in exposure routes (i.e., waterborne vs. enriched food), exposure duration (24 h vs. 28 days), polymer type (PMMA vs. PS), and particle surface functionalization (plain vs. -COOH), age of the individual (adult vs. juvenile), techniques used (biochemistry vs. molecular analysis), as well as the tissue target (liver vs. whole body). Finally, the TOSC assays, which aimed to evaluate the overall antioxidant system's ability to neutralize two potent cellular oxidants (peroxyl and hydroxyl radicals), also showed no statistical differences.

4.2. IBRv2i and Cliff's Delta as Sensitive Tools for the Detection and Description of Slight Responses

IBRv2i was only recently proposed (in 2024) and represents an updated version of the IBR index. One of the main advantages of this new version is the ability to calculate values on a replica-by-replica basis, avoiding the use of pseudo-replicates as proposed by Devin et al. [69]. This enables the application of subsequent hypothesis testing analysis to assess potential differences between experimental groups, making the analyses more robust. In this study, the application of this index allowed for the detection of differences, including statistically significant ones, between animals exposed to NPs and the control group, demonstrating its potential as a promising, consistent, and sensitive tool. This is particularly relevant in cases where individual biomarker responses are borderline and/or masked, for example, by high inter-replica variability (as observed in our case). Furthermore, its use appears to be particularly effective when combined with Cliff's delta calculation. Cliff's delta measures the degree of non-overlap between the response distributions of the tested and control groups. Negative values indicate a lower response in the tested group compared to the control, while positive values suggest greater biomarker activation in the tested group than in the control. The combination of Cliff's delta calculation with a heatmap thus provides a clear visual representation of biomarker activation patterns, which, in our case, primarily involve the activation and production of the enzyme catalase, the inhibition of glutathione S-transferase, and higher values in TOSC ROO assay. CAT catalyzes the decomposition of hydrogen peroxide to produce water and molecular oxygen. It is an enzyme that acts quickly and is specific for the neutralization of hydrogen peroxide. Increased levels of CAT are thus indicative of a quick and early response to oxidative stress. Glutathione S-transferases are a group of Phase II enzymes that conjugate glutathione (GSH) to toxic substances in order to facilitate their elimination [54]. The inhibition of GST activity can occur in case of excess [55] or chronic [56] stress when the GSH has been depleted. TOSCA is an effect biomarker, useful for the quantification of the total oxidant scavenging capacity of antioxidants. Thus, the higher values reported in high treatment of this study can be indicative of the onset of impairment in the defense systems.

4.3. Transcriptomics

The number of differentially expressed (DE) genes identified in *Amphiprion ocellaris* juveniles following PS-NP exposure was lower than that reported in comparable studies with zebrafish [45]. This difference may, in part, be attributed to the comparatively less comprehensive genome annotation of *A. ocellaris*, which could limit the detection and functional characterization of DE genes. Additionally, species-specific physiological and

genetic responses, as well as experimental design factors such as exposure duration, concentration, and developmental stage, may have contributed to the observed variation in transcriptomic responses. Nonetheless, the findings of this study offer several noteworthy insights, discussed below.

4.3.1. Oxidative Stress and Antioxidant Defenses

A unifying theme in the clownfish's response is oxidative stress. Nanoplastics are known to induce reactive oxygen species generation and oxidative damage in aquatic organisms. Our findings support this: the enrichment of hydrogen peroxide metabolic processes and up-regulation of H_2O_2-catabolizing proteins indicate activation of antioxidant defenses. Notably, the globin genes induced at high concentration may function analogously to known antioxidant enzymes [70]. In fish, hemoglobin and myoglobin derivatives (and related globins like cytoglobins) can play roles in ROS scavenging, mitigating oxidative damage during stress [71–73]. The transcriptomic data therefore suggest that high NP exposure imposed significant oxidative pressure on clownfish tissues, to which the fish responded by elevating expression of ROS-neutralizing factors. This aligns with previous studies in zebrafish larvae and adults that reported up-regulation of oxidative stress pathways upon MP or NP exposure. For instance, Brun et al. [74] noted that NPs exposure in zebrafish activated genes associated with oxidative stress and other stress responses. Moreover, investigations in microplastics toxicology in fish concludes that oxidative stress is a hallmark of microplastics exposure, often evidenced by increased antioxidant enzyme activity and transcription of stress biomarkers [75,76]. In *A. ocellaris*, the transcriptional activation of H_2O_2-degrading processes confirms that similar mechanisms are at play in a marine reef fish, underlining oxidative stress as a conserved response to micro- and nanoplastic pollution across diverse fish species.

4.3.2. Metabolic and Physiological Adjustments

The observed changes in metabolic gene expression in clownfish suggest that nanoplastic exposure disrupts energy homeostasis and nutrient metabolism. The up-regulation of *soat2* implicates altered lipid metabolism, particularly cholesterol esterification. This may reflect a need to remodel cellular membranes, potentially to maintain membrane integrity under stress, or an attempt to sequester excess cholesterol or fat-soluble toxins [77–79]. Supporting this, transcriptomic analyses in zebrafish have similarly reported significant down-regulation of lipid metabolism pathways following polyethylene and polystyrene MP exposure, alongside alterations in energy utilization and storage [77].

In our clownfish dataset, the up-regulation of *soat2* also indicates perturbed lipid processing. While the direction of change differs (up-regulation vs. down-regulation), both studies highlight the disruptive impact of NP- and MPs on metabolic homeostasis. It is plausible that clownfish increase *soat2* expression to compensate for impaired dietary lipid absorption or to counteract membrane oxidative damage by accelerating membrane lipid turnover.

Concurrently, the induction of *ampd3b* suggests a shift in energy metabolism, potentially through activation of the purine nucleotide cycle to support ATP regeneration under stress [80,81]. Collectively, these transcriptional changes point to a state of metabolic reorganization in MP-exposed fish, wherein energy production pathways and substrate usage are reprogrammed to meet the elevated demands of cellular stress responses, such as antioxidant defense, tissue repair, or coping with reduced nutrient assimilation due to gut perturbation.

4.3.3. Muscle Function and Oxygen Transport

Transcriptomic evidence indicating modulation of muscle-related genes (e.g., *troponin* genes and *s100a1*) and the strong induction of oxygen transport genes at high NP concentration points to potential impacts on the cardiovascular and muscular systems of *A. ocellaris*. One plausible explanation is that NP exposure may impose a state of mild hypoxic stress [82], possibly due to impaired gill function or increased oxygen demand to counteract stress, thereby potentially stimulating erythropoietin-related pathways or enhancing blood oxygen-carrying capacity. The up-regulation of hemoglobin-like genes at high concentrations may reflect a hypoxia-like response aimed at maintaining adequate oxygen delivery. However, unlike classical hypoxia, which typically involves stabilization of HIF1α and induction of erythropoietin, the driving factor here may be systemic stress initiated by NP toxicity.

The concurrent induction of muscle contraction genes, such as *troponin* genes, may represent a compensatory mechanism to sustain cardiac output and muscular efficiency under conditions of potential hypoxemia or oxidative stress [83]. *Troponin T* and *I* are essential for muscle contractility, and their increased expression may reflect muscle remodeling or an effort to preserve contractile function in a stressed physiological state[84–86].

Notably, similar effects have been observed in zebrafish exposed chronically to microplastics, where reduced swimming activity and mild cardiotoxicity were reported. In that study, zebrafish exhibited inflammation in gill and gut tissues, along with slight impairment of muscular enzymes, including mild inhibition of acetylcholinesterase [87–89]. In contrast, *A. ocellaris* appears to mount a transcriptional response that reinforces its contractile machinery, possibly to mitigate comparable functional stress.

However, the pronounced down-regulation of *s100a1* at low concentration suggests early disruption of calcium handling in muscle. *s100a1* plays a critical role in calcium cycling within cardiac tissue, and its suppression may lead to reduced contractile vigor or increased susceptibility to arrhythmias [90–92]. Interestingly, *s100a1* expression returned to baseline at the high concentration, suggesting a complex, non-linear concentration–response relationship. This pattern may indicate that moderate stress disrupts calcium signaling transiently, while severe stress activates alternative pathways that either mask the effect or engage feedback mechanisms restoring *s100a1* expression.

Collectively, these findings suggest that NPs can subtly impair muscular function, with the organism attempting to compensate through targeted gene expression changes. Whether these compensatory mechanisms are sufficient to prevent physiological deficits remains an open question.

4.3.4. Concentration-Dependent Transcriptomic Response

The magnitude of the molecular response in *A. ocellaris* scaled clearly with NP concentration. Both treatments produced a broad "nanoplastic-stress signature" of 120 genes that shifted in the same direction at 20 $\mu g\ L^{-1}$ and 2000 $\mu g\ L^{-1}$, yet the size of the response and the pathways involved diverged markedly beyond this shared core.

At the environmentally realistic concentration (low group), the transcriptome pointed to subtle but coordinated acclimatory changes. Roughly two-thirds of DEGs were up-regulated, and functional enrichment was dominated by visual and sensory categories such as "lens development", "visual perception", and the molecular function "structural constituent of eye lens". These shifts likely enhance photo-protection or lens maintenance to offset mild oxidative or metabolic stress. A small set of contractile-fiber genes and metabolic regulators was also induced, suggesting energy mobilization for repair, while the down-regulation of calcium-handling protein *s100a1* hints at transient repression of excitation–contraction coupling to conserve resources. Collectively, the low-concentration

profile resembles an early-warning, energy-reallocation program aimed at preserving essential sensory performance while minimizing expendable functions.

The severe exposure (high group) amplified the shared stress signature and recruited an additional 289 unique genes, producing pronounced enrichment of "muscle contraction", "oxygen transport", "hydrogen-peroxide catabolism", and extracellular-matrix terms. Up-regulation of multiple hemoglobin subunit genes, as well as myoglobin and cytoglobin, suggests a physiological response to hypoxia-like stress. This pattern is consistent with known adaptation strategies in teleosts, including increased erythropoiesis, expression of high-affinity globin isoforms, and induction of tissue-specific globins [93,94]. In clownfish, the concerted rise in *hb*, *mb*, and *cygb2* transcripts likely reflects increased oxygen demand caused by gill irritation or particle aggregation impairing respiration. Concomitant induction of antioxidant globins and hydrogen peroxide-detoxifying enzymes supports the presence of a strong oxidative challenge. Although blood parameters were not measured, the transcriptomic signal aligns with a canonical hypoxia response seen in other species. For example, in red drum (*Sciaenops ocellatus*), chronic hypoxia leads to differential expression of hemoglobin isoforms with higher oxygen affinity [93]. In zebrafish, acute hypoxia modulates globin gene expression by initially suppressing some *hb* isoforms while inducing myoglobin and neuroglobin in the heart and brain [94], followed by increased red blood cell production with prolonged exposure [95].

Myoglobin, predominantly expressed in cardiac and skeletal muscle, acts as an oxygen buffer and facilitator of O_2 diffusion [96]. Notably, *myoglobin* also scavenges reactive oxygen species (ROS) and nitric oxide (NO), contributing to cellular protection under oxidative stress [97,98]. Similarly, *cytoglobin*, a globin expressed in fibroblasts, liver, and brain, plays a role in detoxifying ROS and modulating NO availability. In zebrafish, loss of *cygb1* leads to lipid peroxidation and cellular injury under stress, confirming its cytoprotective function [99]. Parallel over-expression of collagen isoforms and other ECM components signals active tissue remodeling or incipient fibrosis, consistent with inflammatory or reparative processes in damaged epithelia [100]. Muscle-specific transcripts (*troponin* and *myosin genes*) were further boosted, plausibly to support higher ventilatory and circulatory workload under stress [101]. Unlike the low concentration, *s100a1* expression returned to baseline, suggesting that beyond a threshold of damage, the fish mobilize alternative calcium-handling pathways to preserve contractility.

Together with classical antioxidant enzymes, the induction of these globins reflects an integrated strategy to enhance oxygen delivery and limit oxidative damage. This dual function, transporting O_2 and neutralizing ROS/NO, is documented in other species. In common carp (*Cyprinus carpio*) upregulate *myoglobin* isoform protect vital tissues during near-anoxic conditions [102].

Although clownfish may not match such hypoxia tolerance, their transcriptional profile under high NP exposure mirrors the general teleost response to oxygen limitation: upregulating *hb* for better oxygen transport [103], activating *mb* and *cygb* for local buffering and redox balance [104], highlights a coordinated effort to restore oxygen homeostasis and prevent oxidative injury.

While details vary across species, e.g., red drum favor isoform switching [93], zebrafish elevate *neuroglobin* [94], and goldfish depress metabolism, the unifying theme remains: diverse teleosts deploy globin-based and antioxidant strategies to withstand oxygen stress [105,106]. Clownfish appear to engage similar pathways, emphasizing the conserved nature of the hypoxic stress response toolkit in fish.

Despite distinct pathway footprints, fold-change values for the 120 shared DEGs were positively correlated across concentrations, with most genes showing larger amplitudes at 2000 μg L^{-1} but maintaining directionality. This indicates that the low-concentra-

tion response is not separate in nature but rather a subdued precursor of the high-concentration program. The shift from sensory-metabolic tuning at 20 μg L^{-1} to intense oxygen-delivery, antioxidant and ECM-remodeling activity at 2000 μg L^{-1} mirrors classic toxicological patterns in which mild exposure triggers compensatory pathways, whereas higher burdens engage defense and repair systems essential for survival.

Juvenile clownfish react to nanoplastic stress along a concentration gradient with early sensory and metabolic adjustments, giving way to a robust hypoxia-oxidative-fibrotic axis as particle burden intensifies. These findings refine our understanding of concentration-dependent plastic toxicity in reef fishes and underscore the importance of considering environmentally relevant exposures alongside worst-case scenarios.

4.4. Functional Implications

The enriched Gene Ontology terms and the identity of DE genes indicate several interconnected stress response mechanisms. At the high exposure concentration (2000 μg/L), a pronounced transcriptional response emerged, involving genes associated with muscle function, oxidative stress responses, oxygen transport, and extracellular matrix (ECM) remodeling. The upregulation of oxygen transporter genes suggests that clownfish exposed to NPs may experience hypoxia-like conditions or an increased tissue oxygen demand, potentially resulting from physical interference or oxidative damage to gill tissues, necessitating compensatory hemoglobin synthesis. Interestingly, these globin genes are also implicated in hydrogen peroxide breakdown, indicating a role in oxidative stress mitigation by degrading reactive peroxides and protecting tissues ([107,108]). Further supporting this, additional DE genes such as *ampd3b* and *soat2* indicate broader cellular stress responses, influencing energy metabolism and lipid homeostasis, respectively [47,109–111].

Marked upregulation of collagen genes (*Col1a1*, *Col11a1*) and other ECM components reflects significant shifts towards tissue remodeling or fibrosis, complementing biochemical findings of inflammation and cellular stress [112]. Such ECM remodeling, although initially protective, could lead to pathological alterations and impaired tissue functionality over prolonged exposures [113], paralleling chronic effects documented for microplastics [114].

A particularly robust induction of *bglap* (osteocalcin), involved in bone metabolism, points toward potential endocrine disruption or aberrant calcium metabolism [115]. Osteocalcin expression might indicate disturbed mineral homeostasis or ectopic bone-like responses, reinforcing systemic endocrine and metabolic perturbations caused by NPs.

Although GO enrichment analysis for the low-concentration group (20 μg/L) did not yield significant categories at the selected threshold, likely due to the moderate number of DE genes and their functional diversity, many of the biological processes significantly affected in the high-concentration group (e.g., muscle contraction, oxygen transport) showed similar trends in the low-concentration group, albeit with weaker responses. In contrast, low-concentration exposure elicited significant transcriptomic changes dominated by sensory and visual system genes.

One of the most striking responses observed at low NP concentration was the coordinated upregulation of several crystallin genes (e.g., *cryaa*, *crybb1*, *cryba4*), which represent the major structural proteins of the vertebrate lens [116]. While their primary role is to maintain lens transparency and refractive properties, crystallins—especially α-crystallins—also act as molecular chaperones with heat-shock–like activity, stabilizing proteins under oxidative stress conditions [117]. In vertebrates, α-crystallins (αA and αB) are members of the small heat shock protein (sHSP) family that bind partially unfolded proteins and prevent their aggregation, thereby maintaining proteostasis in stressed cells [118–120].

In teleosts, the crystallin domain family is expressed not only in the eye lens but also, at lower levels, in extraocular tissues such as the retina, nervous system, and muscle, where they may exert protective functions [121–123]. Studies in various aquatic models have confirmed that α-crystallins are responsive to heat [124], oxidative insult [125], and neurotoxicants [120,126], and that their upregulation reduces apoptosis and preserves tissue integrity [127,128]. The αB-crystallin paralog *cryabb*, in particular, is broadly expressed in various tissues in zebrafish, and has been shown to act as a mitochondrial stabilizer and ROS scavenger during toxicant exposure [125,129]. The evolutionary expansion and tissue-specific expression of α-crystallins in teleosts suggest that their role has diversified beyond structural lens function to include more general stress resilience mechanisms [130].

Their enrichment in our dataset suggests that PS-NP exposure activates multi-level protective pathways, with α-crystallins acting as chaperones to limit protein damage. Interestingly, the transcriptional activation of crystallins occurred in parallel with the upregulation of retinol-binding protein 3 (RBP3). RBP3 is a key interphotoreceptor retinoid-binding protein that shuttles vitamin A derivatives between photoreceptors and the retinal pigment epithelium, ensuring the regeneration of visual pigments [131]. Beyond its canonical transport function, RBP3 has also been shown to provide antioxidant protection within the interphotoreceptor matrix [132].

In teleosts, RBP3 biology presents unique features that may further enhance its importance under NP stress. The *rbp3* gene has undergone lineage-specific duplication, giving rise to *rbp3* and an "irbp-like" paralog (*irbpl*) in species such as zebrafish [133]. While both encode large retinoid-binding proteins, their expression domains have diverged: canonical *rbp3* is localized mainly in photoreceptors and the retinal pigment epithelium, whereas *irbpl* is enriched in the pineal complex and inner retinal layers, with reduced expression in ganglion cells [133]. This sub-functionalization indicates that teleosts deploy distinct retinoid-binding proteins to sustain retinoid cycling in both visual and non-visual photoreceptive organs.

Within the interphotoreceptor matrix, RBP3 proteins not only shuttle all-trans retinol from photoreceptors to the pigment epithelium and return 11-cis retinol [134,135] but also protect these retinoids from oxidation through thiol-dependent antioxidant activity [136,137]. These dual functions make RBP3 indispensable for retinal homeostasis, as demonstrated by vertebrate loss-of-function studies. Moreover, RBP3 modulation has been linked to developmental transitions. In the Japanese flounder (*Paralichthys olivaceus*), transcriptomic analyses revealed differential *rbp3* expression during metamorphosis, coinciding with asymmetric eye migration and activation of retinoic acid pathways [138]. Although this reflects a lineage-specific program, it highlights the broader developmental relevance of RBP3 in teleosts. In contrast, other tissues such as liver, brain, and gonads show little to no RBP3 expression, reinforcing its functional specialization to ocular and pineal tissues.

The simultaneous induction of crystallins and RBP3 at low NP concentrations can therefore be interpreted as a concerted early-warning strategy that prioritizes the preservation of sensory capacity. In coral reef fishes such as *A. ocellaris*, vision is essential for survival, mediating predator avoidance, host-anemone recognition, and social interactions [139]. The observed transcriptional response suggests that even sub-toxic NP levels are sufficient to mobilize protective programs in ocular tissues, highlighting the vulnerability of visual systems to nanoplastic stress. Such prioritization of sensory maintenance, potentially at the expense of metabolic or digestive functions that appeared downregulated, reflects a strategic reallocation of resources to safeguard ecologically critical functions.

Finally, crystallins belong to an ancient and highly conserved protein superfamily, with structural and chaperone roles that extend beyond the vertebrate eye [116]. Their

recruitment in response to NP exposure may represent a generalizable mechanism of protein homeostasis under stress [140]. Combined with the antioxidant properties and evolutionary diversification of RBP3 in teleosts, this concerted induction underscores the importance of oxidative stress as a central driver of NP toxicity. Future work should explore whether crystallin and RBP3 induction represent a common biomarker signature across marine teleosts, providing mechanistic insight into the long-term impacts of nanoplastics on fish sensory ecology.

In conclusion, exposure to polystyrene NPs elicited a suite of transcriptomic changes in clownfish juveniles indicative of physiological stress. These include activation of antioxidant defenses, modulation of oxygen transport and utilization, and adjustments in muscle function and metabolic regulation.

4.5. Ecotoxicological Implications

The transcriptomic changes observed in clownfish have important biological and ecological implications. Evidence of oxidative stress and the activation of protective pathways suggests that NP exposure, even at sub-lethal levels, imposes a physiological cost on the organism. Chronic oxidative stress can lead to macromolecular damage, accelerated cellular aging, or apoptosis if antioxidant defenses are overwhelmed [50,77,141]. Although our short-term exposure elicited compensatory up-regulation of antioxidant genes, prolonged exposure to nanoplastic pollution could deplete these defenses, potentially resulting in pathological outcomes such as tissue damage or organ dysfunction.

Alterations in muscle-related gene expression point to possible impacts on locomotor performance and cardiovascular function. In natural environments, even mild impairments in swimming ability or cardiac output could diminish a fish's capacity to forage, evade predators, or reproduce successfully. Concurrent changes in metabolic enzymes and pathways further suggest that energy resources may be reallocated from growth and reproduction toward cellular maintenance and stress mitigation. Supporting this, studies in medaka have reported growth retardation and delayed hatching in populations exposed to microplastics [142,143]. If *A. ocellaris* similarly diverts energy to cope with nanoplastic-induced stress, reduced growth rates and fecundity may result.

Over time, these sub-lethal effects could scale to population-level consequences, including diminished recruitment and altered age structure. Ecologically, clownfish play a key role in coral reef ecosystems through their mutualistic association with sea anemones and their contribution to reef biodiversity. Compromised health in clownfish due to nanoplastic exposure could disrupt these interactions and serve as an early indicator of pollution stress within reef environments.

Notably, the pronounced activation of oxygen transport pathways in clownfish may reflect a species-specific response, potentially linked to their physiology or habitat. Clownfish inhabit reef lagoons and live in close association with anemones, environments where diel oxygen fluctuations, especially nocturnal hypoxia, are common. Thus, their strong erythropoietin response to nanoplastic stress may represent a pre-adapted trait that becomes amplified under pollutant-induced strain.

5. Conclusions

The integration of our findings with existing knowledge from zebrafish and medaka models paints a consistent narrative: nanoplastics elicit oxidative stress, metabolic and physiological reorganization, and potential immune disturbances in fish, ultimately threatening organismal health and ecosystem stability if exposure persists. Each model, from freshwater to marine, adds a piece to this puzzle, and *Amphiprion ocellaris* now stands out as a key piece representing the marine vertebrate response.

The extensive transcriptomic changes documented (across hundreds of genes and multiple pathways) highlight that even short-term nanoplastic exposure can perturb biological systems at a molecular level. In conclusion, the transcriptomic responses in *A. ocellaris* illuminate the cascade of cellular stress and adaptation mechanisms triggered by nanoplastics, providing a detailed picture of how these pollutants affect marine fish health. These insights not only advance our scientific understanding of nanoplastic toxicity but also reinforce the ecological urgency of addressing plastic pollution for the sake of maintaining healthy marine ecosystems.

Supplementary Materials: The following supporting information can be downloaded at: https://www.mdpi.com/article/10.3390/microplastics5010014/s1, Figure S1: Image of the nanoplastics tested in the experiment, captured by the Transmission Electron Microscope (magnification 20,000×, voltage 100 kV). The average particle size, measured on 30 beads using ImageJ software v. 1.8.0, was 97 ± 4 nm (mean ± standard deviation), consistent with the supplier's specifications; Figure S2: DLS analysis indicates optimal dispersion of PS-NPs at (a) 200 μg/L and (b) 2000 μg/L (high treatment) concentrations in Milli-Q water, with no significant changes over time. In contrast, PS-NPs dispersed in ASW exhibited a higher Z-average and PdI, suggesting an aggregation pattern. Data for the low concentration (20 μg/L) are unavailable due to the technological limitations of the instrument; Figure S3: Non-metric MDS based on all transcripts with TPM > 1; Table S1: GO enrichment analysis for exposure to low NP concentration (20 μg/L). Significantly enriched Gene Ontology (GO) terms related to Biological Process and Molecular Function are reported, along with the associated genes (only terms with observed gene counts > 3 and FDR ≤ 0.05 are shown). GO terms under the Cellular Component category are not included, as no highly significant enrichment was observed in that category; Table S2: GO enrichment analysis for exposure to high NP concentration (2000 μg/L). Significantly enriched Gene Ontology (GO) terms related to Biological Process, Molecular Function, and cellular Component are reported, along with the associated genes (only terms with observed gene counts > 3 and FDR ≤ 0.05 are shown) [144–146].

Author Contributions: Conceptualization, M.P., P.S. and A.T.; methodology, M.P., P.S. and A.T.; validation, P.D.L., M.R. and S.G.; formal analysis, M.P., M.M. and A.P.; investigation, M.P., L.P. and R.M.S.; resources, S.G. and V.L.; data curation, A.P.; writing—original draft preparation, M.P. and M.M.; writing—review and editing, all authors; visualization, M.P.; supervision, L.B., P.S. and A.T.; funding acquisition, V.L., P.S. and A.T. All authors have read and agreed to the published version of the manuscript.

Funding: The research leading to these results received funding, or partial funding, from the European Union's Horizon 2020 research and innovation program under grant agreement No 730984, ASSEMBLE Plus project and from the National Biodiversity Future Centre (NBFC) Program, Italian Ministry of University and Research, PNRR, Missione 4 Componente 2 Investimento 1.4 (Project: CN00000033). This study is part of Manuela Piccardo's PhD scholarship funded by the University of Trieste and Stazione Zoologica Anton Dohrn.

Institutional Review Board Statement: All experiments were performed according to the European Union regulations concerning the protection of experimental animals. Animal experimental protocols were approved by the Animal Care and Use Committee of the Observatoire Océanologique of Banyuls sur Mer (CNRS-UPMC; authorization # A-66-01-601).

Data Availability Statement: The transcriptomic dataset generated in this study will be deposited in Zenodo and made publicly available upon acceptance of the manuscript at the following DOI: https://doi.org/10.5281/zenodo.17432021.

Acknowledgments: We thank Francesca Capanni for her precious support in the preliminary bioinformatics analyses. The graphical abstract was created in BioRender. Bevilacqua, S. (2025) https://BioRender.com/v8xpiqe.

Conflicts of Interest: The authors declare no conflicts of interest.

References

1. Plastic Europe. *Plastics—The fast Facts 2023*; Plastic Europe: Brussels, Belgium, 2023.
2. Jambeck, J.R.; Geyer, R.; Wilcox, C.; Siegler, T.R.; Perryman, M.; Andrady, A.; Narayan, R.; Law, K.L. Plastic waste inputs from land into the ocean. *Science* **2015**, *347*, 768–771. https://doi.org/10.1126/science.1260352.
3. Geyer, R.; Jambeck, J.R.; Law, K.L. Production, use, and fate of all plastics ever made. *Sci. Adv.* **2017**, *3*, e1700782. https://doi.org/10.1126/sciadv.1700782.
4. Bergmann, M.; Gutow, L.; Klages, M. (Eds.) *Marine Anthropogenic Litter*; Springer Nature: New York, NY, USA, 2015; p. 447. https://doi.org/10.1007/978-3-319-16510-3.
5. Gewert, B.; Plassmann, M.M.; MacLeod, M. Pathways for degradation of plastic polymers floating in the marine environment. *Environ. Sci. Process. Impacts* **2015**, *17*, 1513–1521. https://doi.org/10.1039/c5em00207a.
6. Potthoff, A.; Oelschlägel, K.; Schmitt-Jansen, M.; Rummel, C.D.; Kühnel, D. From the Sea to the Laboratory: Characterization of Microplastic as Prerequisite for the Assessment of Ecotoxicological Impact. *Integr. Environ. Assess. Manag.* **2017**, *13*, 500–504. https://doi.org/10.1002/ieam.1902.
7. Thompson, R.C.; Courtene-Jones, W.; Boucher, J.; Pahl, S.; Raubenheimer, K.; Koelmans, A.A. Twenty years of microplastic pollution research—What have we learned? *Science* **2024**, *386*, eadl2746. https://doi.org/10.1126/science.adl2746.
8. Alimi, O.S.; Farner Budarz, J.; Hernandez, L.M.; Tufenkji, N. Microplastics and Nanoplastics in Aquatic Environments: Aggregation, Deposition, and Enhanced Contaminant Transport. *Environ. Sci. Technol.* **2018**, *52*, 1704–1724. https://doi.org/10.1021/acs.est.7b05559.
9. Azimi, P.; Zhao, D.; Pouzet, C.; Crain, N.E.; Stephens, B. Emissions of Ultrafine Particles and Volatile Organic Compounds from Commercially Available Desktop Three-Dimensional Printers with Multiple Filaments. *Environ. Sci. Technol.* **2016**, *50*, 1260–1268. https://doi.org/10.1021/acs.est.5b04983.
10. Hernandez, L.M.; Yousefi, N.; Tufenkji, N. Are There Nanoplastics in Your Personal Care Products? *Environ. Sci. Technol. Lett.* **2017**, *4*, 280–285. https://doi.org/10.1021/acs.estlett.7b00187.
11. Ter Halle, A.; Jeanneau, L.; Martignac, M.; Jardé, E.; Pedrono, B.; Brach, L.; Gigault, J. Nanoplastic in the North Atlantic Subtropical Gyre. *Environ. Sci. Technol.* **2017**, *51*, 13689–13697. https://doi.org/10.1021/acs.est.7b03667.
12. Materić, D.; Holzinger, R.; Niemann, H. Nanoplastics and ultrafine microplastic in the Dutch Wadden Sea—The hidden plastics debris? *Sci. Total. Environ.* **2022**, *846*, 157371. https://doi.org/10.1016/j.scitotenv.2022.157371.
13. Materić, D.; Kasper-Giebl, A.; Kau, D.; Anten, M.; Greilinger, M.; Ludewig, E.; van Sebille, E.; Röckmann, T.; Holzinger, R. Micro- and Nanoplastics in Alpine Snow: A New Method for Chemical Identification and (Semi)Quantification in the Nanogram Range. *Environ. Sci. Technol.* **2020**, *54*, 2353–2359. https://doi.org/10.1021/acs.est.9b07540.
14. Sullivan, G.; Gallardo, J.D.; Jones, E.; Hollliman, P.; Watson, T.; Sarp, S. Detection of trace sub-micron (nano) plastics in water samples using pyrolysis-gas chromatography time of flight mass spectrometry (PY-GCToF). *Chemosphere* **2020**, *249*, 126179. https://doi.org/10.1016/j.chemosphere.2020.126179.
15. Materić, D.; Peacock, M.; Dean, J.; Futter, M.N.; Maximov, T.; Moldan, F.; Roeckmann, T.; Holzinger, R. Presence of nanoplastics in rural and remote surface waters. *Environ. Res. Lett.* **2022**, *17*, 054036. https://doi.org/10.1088/1748-9326/ac68f7.
16. Wahl, A.; Le Juge, C.; Davranche, M.; El Hadri, H.; Grassl, B.; Reynaud, S.; Gigault, J. Nanoplastic occurrence in a soil amended with plastic debris. *Chemosphere* **2021**, *262*, 127784. https://doi.org/10.1016/j.chemosphere.2020.127784.
17. Plastic Europe. *Plastics—The Facts 2022*; Plastic Europe: Brussels, Belgium, 2022.
18. Shim, W.; Hong, S.; Jang, M.; Han, G. Producing fragmented micro- and nano-sized expanded polystyrene particles with an accelerated mechanical abrasion experiment. In Proceedings of the Science Across Bridges, Borders and Boundaries—Abstract Book—SETAC Europe 24th Annual Meeting, Basel, Switzerland, 11–15 May 2014; p. 122. https://doi.org/10.13140/RG.2.2.20991.61602.
19. Gigault, J.; Pedrono, B.; Maxit, B.; Ter Halle, A. Marine plastic litter: The unanalyzed nano-fraction. *Environ. Sci. Nano* **2016**, *3*, 346–350. https://doi.org/10.1039/c6en00008h.
20. Song, Y.K.; Hong, S.H.; Jang, M.; Han, G.M.; Jung, S.W.; Shim, W.J. Combined Effects of UV Exposure Duration and Mechanical Abrasion on Microplastic Fragmentation by Polymer Type. *Environ. Sci. Technol.* **2017**, *51*, 4368–4376. https://doi.org/10.1021/acs.est.6b06155.
21. Lambert, S.; Wagner, M. Characterisation of nanoplastics during the degradation of polystyrene. *Chemosphere* **2016**, *145*, 265–268. https://doi.org/10.1016/j.chemosphere.2015.11.078.

22. Liu, J.; Zhang, T.; Tian, L.; Liu, X.; Qi, Z.; Ma, Y.; Ji, R.; Chen, W. Aging Significantly Affects Mobility and Contaminant-Mobilizing Ability of Nanoplastics in Saturated Loamy Sand. *Environ. Sci. Technol.* **2019**, *53*, 5805–5815. https://doi.org/10.1021/acs.est.9b00787.
23. Piccardo, M.; Renzi, M.; Terlizzi, A. Nanoplastics in the oceans: Theory, experimental evidence and real world. *Mar. Pollut. Bull.* **2020**, *157*, 111317. https://doi.org/10.1016/j.marpolbul.2020.111317.
24. Chae, Y.; Kim, D.; Kim, S.W.; An, Y.-J. Trophic transfer and individual impact of nano-sized polystyrene in a four-species freshwater food chain. *Sci. Rep.* **2018**, *8*, 284. https://doi.org/10.1038/s41598-017-18849-y.
25. Pitt, J.A.; Kozal, J.S.; Jayasundara, N.; Massarsky, A.; Trevisan, R.; Geitner, N.; Wiesner, M.; Levin, E.D.; Di Giulio, R.T. Uptake, tissue distribution, and toxicity of polystyrene nanoparticles in developing zebrafish (*Danio rerio*). *Aquat. Toxicol.* **2018**, *194*, 185–194. https://doi.org/10.1016/j.aquatox.2017.11.017.
26. Cedervall, T.; Hansson, L.A.; Lard, M.; Frohm, B.; Linse, S. Food Chain Transport of Nanoparticles Affects Behaviour and Fat Metabolism in Fish. *PLoS ONE* **2012**, *7*, e32254. https://doi.org/10.1371/journal.pone.0032254.
27. Bhagat, J.; Zang, L.; Nishimura, N.; Shimada, Y. Zebrafish: An emerging model to study microplastic and nanoplastic toxicity. *Sci. Total. Environ.* **2020**, *728*, 138707. https://doi.org/10.1016/j.scitotenv.2020.138707.
28. Chen, Q.; Gundlach, M.; Yang, S.; Jiang, J.; Velki, M.; Yin, D.; Hollert, H. Quantitative investigation of the mechanisms of microplastics and nanoplastics toward zebrafish larvae locomotor activity. *Sci. Total. Environ.* **2017**, *584*, 1022–1031. https://doi.org/10.1016/j.scitotenv.2017.01.156.
29. Brandts, I.; Teles, M.; Tvarijonaviciute, A.; Pereira, M.; Martins, M.; Tort, L.; Oliveira, M. Effects of polymethylmethacrylate nanoplastics on *Dicentrarchus labrax*. *Genomics* **2018**, *110*, 435–441. https://doi.org/10.1016/j.ygeno.2018.10.006.
30. Brandts, I.; Barría, C.; Martins, M.; Franco-Martínez, L.; Barreto, A.; Tvarijonaviciute, A.; Tort, L.; Oliveira, M.; Teles, M. Waterborne exposure of gilthead seabream (*Sparus aurata*) to polymethylmethacrylate nanoplastics causes effects at cellular and molecular levels. *J. Hazard. Mater.* **2021**, *403*, 123590. https://doi.org/10.1016/j.jhazmat.2020.123590.
31. Yin, L.; Liu, H.; Cui, H.; Chen, B.; Li, L.; Wu, F. Impacts of polystyrene microplastics on the behavior and metabolism in a marine demersal teleost, black rockfish (*Sebastes schlegelii*). *J. Hazard. Mater.* **2019**, *380*, 120861. https://doi.org/10.1016/j.jhazmat.2019.120861.
32. Ollerton, J.; McCollin, D.; Fautin, D.G.; Allen, G.R. Finding NEMO: Nestedness engendered by mutualistic organization in anemonefish and their hosts. *Proc. R. Soc. B Biol. Sci.* **2007**, *274*, 591–598. https://doi.org/10.1098/rspb.2006.3758.
33. Elliott, J.K.; Mariscal, R.N. Coexistence of nine anemonefish species: Differential host and habitat utilization, size and recruitment. *Mar. Biol.* **2001**, *138*, 23–36. https://doi.org/10.1007/s002270000441.
34. Madhu, R.; Madhu, K.; Retheesh, T. Life history pathways in false clown *Amphiprion ocellaris* Cuvier, 1830: A journey from egg to adult under captive condition. *J. Mar. Biol. Ass. India* **2012**, *54*, 77–90.
35. Weis, J.S.; Weis, P. Tolerance and Stress in a Polluted Environment. *BioScience* **1989**, *39*, 89–95. https://doi.org/10.2307/1310907.
36. Nanninga, G.B.; Scott, A.; Manica, A. Microplastic ingestion rates are phenotype-dependent in juvenile anemonefish. *Environ. Pollut.* **2020**, *259*, 113855. https://doi.org/10.1016/j.envpol.2019.113855.
37. Roux, N.; Logeux, V.; Trouillard, N.; Pillot, R.; Magré, K.; Salis, P.; Lecchini, D.; Besseau, L.; Laudet, V.; Romans, P. A star is born again: Methods for larval rearing of an emerging model organism, the False clownfish *Amphiprion ocellaris*. *J. Exp. Zool. Part B Mol. Dev. Evol.* **2021**, *336*, 376–385. https://doi.org/10.1002/jez.b.23028.
38. Ryu, T.; Herrera, M.; Moore, B.; Izumiyama, M.; Kawai, E.; Laudet, V.; Ravasi, T. A chromosome-scale genome assembly of the false clownfish, *Amphiprion ocellaris*. *G3 Genes Genomes Genetics* **2022**, *12*, jkac074. https://doi.org/10.1093/g3journal/jkac074.
39. Subaramaniyam, U.; Allimuthu, R.S.; Vappu, S.; Ramalingam, D.; Balan, R.; Paital, B.; Panda, N.; Rath, P.K.; Ramalingam, N.; Sahoo, D.K. Effects of microplastics, pesticides and nano-materials on fish health, oxidative stress and antioxidant defense mechanism. *Front. Physiol.* **2023**, *14*, 1217666. https://doi.org/10.3389/fphys.2023.1217666.
40. Mattos, J.J.; Siebert, M.N.; Bainy, A.C.D. Integrated biomarker responses: A further improvement of IBR and IBRv2 indexes to preserve data variability in statistical analyses. *Environ. Sci. Pollut. Res.* **2024**, *31*, 871–881. https://doi.org/10.1007/s11356-023-31255-4.
41. Sanchez, W.; Burgeot, T.; Porcher, J.-M. A novel "Integrated Biomarker Response" calculation based on reference deviation concept. *Environ. Sci. Pollut. Res.* **2013**, *20*, 2721–2725. https://doi.org/10.1007/s11356-012-1359-1.
42. Merrick, B.A. Next-generation sequencing data for use in risk assessment. *Curr. Opin. Toxicol.* **2019**, *18*, 18–26. https://doi.org/10.1016/j.cotox.2019.02.010.

43. Deng, J.; Zeng, X.; Li, J.; Luo, L.; Yang, Y.; Luan, T. Single-cell transcriptomic analysis reveals heterogeneity of the patterns of responsive genes and cell communications in liver cell populations of zebrafish exposed to polystyrene nanoplastics. *Sci. Total. Environ.* **2023**, *889*, 164082. https://doi.org/10.1016/j.scitotenv.2023.164082.
44. Huang, J.-N.; Wen, B.; Xu, L.; Ma, H.-C.; Li, X.-X.; Gao, J.-Z.; Chen, Z.-Z. Micro/nano-plastics cause neurobehavioral toxicity in discus fish (*Symphysodon aequifasciatus*): Insight from brain-gut-microbiota axis. *J. Hazard. Mater.* **2022**, *421*, 126830. https://doi.org/10.1016/j.jhazmat.2021.126830.
45. Pedersen, A.F.; Meyer, D.N.; Petriv, A.-M.V.; Soto, A.L.; Shields, J.N.; Akemann, C.; Baker, B.B.; Tsou, W.-L.; Zhang, Y.; Baker, T.R. Nanoplastics impact the zebrafish (*Danio rerio*) transcriptome: Associated developmental and neurobehavioral consequences. *Environ. Pollut.* **2020**, *266*, 115090. https://doi.org/10.1016/j.envpol.2020.115090.
46. Pang, M.; Wang, Y.; Tang, Y.; Dai, J.; Tong, J.; Jin, G. Transcriptome sequencing and metabolite analysis reveal the toxic effects of nanoplastics on tilapia after exposure to polystyrene. *Environ. Pollut.* **2021**, *277*, 116860. https://doi.org/10.1016/j.envpol.2021.116860.
47. Jiang, Q.; Chen, X.; Jiang, H.; Wang, M.; Zhang, T.; Zhang, W. Effects of Acute Exposure to Polystyrene Nanoplastics on the Channel Catfish Larvae: Insights From Energy Metabolism and Transcriptomic Analysis. *Front. Physiol.* **2022**, *13*, 923278. https://doi.org/10.3389/fphys.2022.923278.
48. Veneman, W.J.; Spaink, H.P.; Brun, N.R.; Bosker, T.; Vijver, M.G. Pathway analysis of systemic transcriptome responses to injected polystyrene particles in zebrafish larvae. *Aquat. Toxicol.* **2017**, *190*, 112–120. https://doi.org/10.1016/j.aquatox.2017.06.014.
49. Auguste, M.; Lasa, A.; Balbi, T.; Pallavicini, A.; Vezzulli, L.; Canesi, L. Impact of nanoplastics on hemolymph immune parameters and microbiota composition in *Mytilus galloprovincialis*. *Mar. Environ. Res.* **2020**, *159*, 105017. https://doi.org/10.1016/j.marenvres.2020.105017.
50. Sun, Z.; Peng, X.; Zhao, L.; Yang, Y.; Zhu, Y.; Wang, L.; Kang, B. From tissue lesions to neurotoxicity: The devastating effects of small-sized nanoplastics on red drum *Sciaenops ocellatus*. *Sci. Total. Environ.* **2024**, *933*, 173238. https://doi.org/10.1016/j.scitotenv.2024.173238.
51. Materić, D.; Kjær, H.A.; Vallelonga, P.; Tison, J.-L.; Röckmann, T.; Holzinger, R. Nanoplastics measurements in Northern and Southern polar ice. *Environ. Res.* **2022**, *208*, 112741. https://doi.org/10.1016/j.envres.2022.112741.
52. Monikh, F.A.; Baun, A.; Hartmann, N.B.; Kortet, R.; Akkanen, J.; Lee, J.-S.; Shi, H.; Lahive, E.; Uurasjärvi, E.; Tufenkji, N.; et al. Exposure protocol for ecotoxicity testing of microplastics and nanoplastics. *Nat. Protoc.* **2023**, *18*, 3534–3564. https://doi.org/10.1038/s41596-023-00886-9.
53. Tan, H.; Mong, G.R.; Wong, S.L.; Wong, K.Y.; Sheng, D.D.C.V.; Nyakuma, B.B.; Othman, M.H.D.; Kek, H.Y.; Razis, A.F.A.; Wahab, N.H.A.; et al. Airborne microplastic/nanoplastic research: A comprehensive Web of Science (WoS) data-driven bibliometric analysis. *Environ. Sci. Pollut. Res.* **2023**, *31*, 109–126. https://doi.org/10.1007/s11356-023-31228-7.
54. Eberhard, T.; Casillas, G.; Zarus, G.M.; Barr, D.B. Systematic review of microplastics and nanoplastics in indoor and outdoor air: Identifying a framework and data needs for quantifying human inhalation exposures. *J. Expo. Sci. Environ. Epidemiol.* **2024**, *34*, 185–196. https://doi.org/10.1038/s41370-023-00634-x.
55. Wang, W.; Mao, X.; Zhang, R.; Zhou, X.-X.; Liu, Y.; Zhou, H.; Jia, J.; Yan, B. Nanoplastic Exposure at Environmental Concentrations Disrupts Hepatic Lipid Metabolism through Oxidative Stress Induction and Endoplasmic Reticulum Homeostasis Perturbation. *Environ. Sci. Technol.* **2023**, *57*, 14127–14137. https://doi.org/10.1021/acs.est.3c02769.
56. Cliff, N. Dominance statistics: Ordinal analyses to answer ordinal questions. *Psychol. Bull.* **1993**, *114*, 494–509. https://doi.org/10.1037/0033-2909.114.3.494.
57. Pham, D.N.; Sokolova, I.M. Dissecting integrated indices of multiple biomarker responses: Think before use. *Integr. Environ. Assess. Manag.* **2022**, *19*, 302–311. https://doi.org/10.1002/ieam.4676.
58. Clarke, K.R.; Gorley, R.N. *PRIMER v7: User Manual/Tutorial. PRIMER-E*; 2015.
59. Piccardo, M.; Bevilacqua, S. Lost in the Dark: Current Evidence and Knowledge Gaps About Microplastic Pollution in Natural Caves. *Environments* **2024**, *11*, 238. https://doi.org/10.3390/environments11110238.
60. Tan, F.; Yang, H.; Xu, X.; Fang, Z.; Xu, H.; Shi, Q.; Zhang, X.; Wang, G.; Lin, L.; Zhou, S.; et al. Microplastic pollution around remote uninhabited coral reefs of Nansha Islands, South China Sea. *Sci. Total. Environ.* **2020**, *725*, 138383. https://doi.org/10.1016/j.scitotenv.2020.138383.
61. Reed, S.; Clark, M.; Thompson, R.; Hughes, K.A. Microplastics in marine sediments near Rothera Research Station, Antarctica. *Mar. Pollut. Bull.* **2018**, *133*, 460–463. https://doi.org/10.1016/j.marpolbul.2018.05.068.

62. Portugal, A.B.; Carvalho, F.L.; Carneiro, P.B.d.M.; Rossi, S.; Soares, M.d.O. Increased anthropogenic pressure decreases species richness in tropical intertidal reefs. *Mar. Environ. Res.* **2016**, *120*, 44–54. https://doi.org/10.1016/j.marenvres.2016.07.005.
63. Ding, J.; Jiang, F.; Li, J.; Wang, Z.; Sun, C.; Wang, Z.; Fu, L.; Ding, N.X.; He, C. Microplastics in the Coral Reef Systems from Xisha Islands of South China Sea. *Environ. Sci. Technol.* **2019**, *53*, 8036–8046. https://doi.org/10.1021/acs.est.9b01452.
64. Garnier, Y.; Jacob, H.; Guerra, A.S.; Bertucci, F.; Lecchini, D. Evaluation of microplastic ingestion by tropical fish from Moorea Island, French Polynesia. *Mar. Pollut. Bull.* **2019**, *140*, 165–170. https://doi.org/10.1016/j.marpolbul.2019.01.038.
65. Guerrera, M.C.; Aragona, M.; Porcino, C.; Fazio, F.; Laurà, R.; Levanti, M.; Montalbano, G.; Germanà, G.; Abbate, F.; Germanà, A. Micro and Nano Plastics Distribution in Fish as Model Organisms: Histopathology, Blood Response and Bioaccumulation in Different Organs. *Appl. Sci.* **2021**, *11*, 5768. https://doi.org/10.3390/app11135768.
66. Birnie-Gauvin, K.; Costantini, D.; Cooke, S.J.; Willmore, W.G. A comparative and evolutionary approach to oxidative stress in fish: A review. *Fish Fish.* **2017**, *18*, 928–942. https://doi.org/10.1111/faf.12215.
67. Pitt, J.A.; Trevisan, R.; Massarsky, A.; Kozal, J.S.; Levin, E.D.; Di Giulio, R.T. Maternal transfer of nanoplastics to offspring in zebrafish (*Danio rerio*): A case study with nanopolystyrene. *Sci. Total. Environ.* **2018**, *643*, 324–334. https://doi.org/10.1016/j.scitotenv.2018.06.186.
68. Wang, Q.; Zuo, Z.; Zhang, C.; Ye, B.; Zou, J. An effect assessment of microplastics and nanoplastics interacting with androstenedione on mosquitofish (*Gambusia affinis*). *Mar. Environ. Res.* **2023**, *189*, 106062. https://doi.org/10.1016/j.marenvres.2023.106062.
69. Devin, S.; Burgeot, T.; Giambérini, L.; Minguez, L.; Pain-Devin, S. The integrated biomarker response revisited: Optimization to avoid misuse. *Environ. Sci. Pollut. Res.* **2014**, *21*, 2448–2454. https://doi.org/10.1007/s11356-013-2169-9.
70. Reeder, B.J. Globin Associated Oxidative Stress. *Antioxidants* **2023**, *12*, 1077. https://doi.org/10.3390/antiox12051077.
71. Maqsood, S.; Benjakul, S.; Kamal-Eldin, A. Haemoglobin-mediated lipid oxidation in the fish muscle: A review. *Trends Food Sci. Technol.* **2012**, *28*, 33–43. https://doi.org/10.1016/j.tifs.2012.06.009.
72. Hematyar, N.; Rustad, T.; Sampels, S.; Dalsgaard, T.K. Relationship between lipid and protein oxidation in fish. *Aquac. Res.* **2019**, *50*, 1393–1403. https://doi.org/10.1111/are.14012.
73. Giordano, D.; Corti, P.; Coppola, D.; Altomonte, G.; Xue, J.; Russo, R.; di Prisco, G.; Verde, C. Regulation of globin expression in Antarctic fish under thermal and hypoxic stress. *Mar. Genom.* **2021**, *57*, 100831. https://doi.org/10.1016/j.margen.2020.100831.
74. Brun, N.R.; van Hage, P.; Hunting, E.R.; Haramis, A.-P.G.; Vink, S.C.; Vijver, M.G.; Schaaf, M.J.M.; Tudorache, C. Polystyrene nanoplastics disrupt glucose metabolism and cortisol levels with a possible link to behavioural changes in larval zebrafish. *Commun. Biol.* **2019**, *2*, 382. https://doi.org/10.1038/s42003-019-0629-6.
75. Félix, L.; Carreira, P.; Peixoto, F. Effects of chronic exposure of naturally weathered microplastics on oxidative stress level, behaviour, and mitochondrial function of adult zebrafish (*Danio rerio*). *Chemosphere* **2023**, *310*, 136895. https://doi.org/10.1016/j.chemosphere.2022.136895.
76. Solomando, A.; Capó, X.; Alomar, C.; Álvarez, E.; Compa, M.; Valencia, J.M.; Pinya, S.; Deudero, S.; Sureda, A. Long-term exposure to microplastics induces oxidative stress and a pro-inflammatory response in the gut of *Sparus aurata* Linnaeus. *Environ. Pollut.* **2020**, *266*, 115295. https://doi.org/10.1016/j.envpol.2020.115295.
77. Limonta, G.; Mancia, A.; Benkhalqui, A.; Bertolucci, C.; Abelli, L.; Fossi, M.C.; Panti, C. Microplastics induce transcriptional changes, immune response and behavioral alterations in adult zebrafish. *Sci. Rep.* **2019**, *9*, 15775. https://doi.org/10.1038/s41598-019-52292-5.
78. Wang, Q.; Wu, Y.; Zhang, W.; Shen, T.; Li, H.; Wu, J.; Zhang, L.; Qin, L.; Chen, R.; Gu, W.; et al. Lipidomics and transcriptomics insight into impacts of microplastics exposure on hepatic lipid metabolism in mice. *Chemosphere* **2022**, *308*, 136591. https://doi.org/10.1016/j.chemosphere.2022.136591.
79. Li, Y.; Ye, Y.; Rihan, N.; Zhu, B.; Jiang, Q.; Liu, X.; Zhao, Y.; Che, X. Polystyrene nanoplastics induce lipid metabolism disorder and alter fatty acid composition in the hepatopancreas of Pacific whiteleg shrimp (*Litopenaeus vannamei*). *Sci. Total. Environ.* **2024**, *906*, 167616. https://doi.org/10.1016/j.scitotenv.2023.167616.
80. Ipata, P.L.; Pesi, R. Metabolic interaction between purine nucleotide cycle and oxypurine cycle during skeletal muscle contraction of different intensities: A biochemical reappraisal. *Metabolomics* **2018**, *14*, 42. https://doi.org/10.1007/s11306-018-1341-0.
81. Kirkwood, J.S.; Lebold, K.M.; Miranda, C.L.; Wright, C.L.; Miller, G.W.; Tanguay, R.L.; Barton, C.L.; Traber, M.G.; Stevens, J.F. Vitamin C Deficiency Activates the Purine Nucleotide Cycle in Zebrafish. *J. Biol. Chem.* **2012**, *287*, 3833–3841. https://doi.org/10.1074/jbc.m111.316018.

82. de Mello, M.M.M.; Piedade, A.E.; Faria, C.d.F.P.d.; Urbinati, E.C. Acute low temperature and lipopolysaccharide differentially modulated the innate immune and antioxidant responses in a subtropical fish, the pacu (*Piaractus mesopotamicus*). *Fish Physiol. Biochem.* **2024**, *51*, 12. https://doi.org/10.1007/s10695-024-01425-3.
83. Johnston, E.F.; Alderman, S.L.; Gillis, T.E. Chronic Hypoxia Exposure of Trout Embryos Alters Swimming Performance and Cardiac Gene Expression in Larvae. *Physiol. Biochem. Zool.* **2013**, *86*, 567–575. https://doi.org/10.1086/672012.
84. Hsiao, C.; Tsai, W.; Horng, L.; Tsai, H. Molecular structure and developmental expression of three muscle-type troponin T genes in zebrafish. *Dev. Dyn.* **2003**, *227*, 266–279. https://doi.org/10.1002/dvdy.10305.
85. Rasmussen, M.; Jin, J.-P. Troponin Variants as Markers of Skeletal Muscle Health and Diseases. *Front. Physiol.* **2021**, *12*, 747214. https://doi.org/10.3389/fphys.2021.747214.
86. Ferrante, M.I.; Kiff, R.M.; Goulding, D.A.; Stemple, D.L. Troponin T is essential for sarcomere assembly in zebrafish skeletal muscle. *J. Cell Sci.* **2011**, *124*, 565–577. https://doi.org/10.1242/jcs.071274.
87. Duan, X.; Helal, M.; Wang, X.; Huang, Y.; Ebbesen, M.F.; Brewer, J.; Wang, S.; Wu, C.; Holbech, H.; Xu, E.G. Swim in Plastics: Clean Nanoplastics Cause Minimal Mortality but Alter Neurobehavioral and Molecular Rhythms in Fish. *Environ. Sci. Technol.* **2025**, *59*, 9387–9398. https://doi.org/10.1021/acs.est.4c10984.
88. Liu, Y.; Wang, Y.; Li, N.; Jiang, S. Avobenzone and nanoplastics affect the development of zebrafish nervous system and retinal system and inhibit their locomotor behavior. *Sci. Total. Environ.* **2022**, *806*, 150681. https://doi.org/10.1016/j.scitotenv.2021.150681.
89. Sarasamma, S.; Audira, G.; Siregar, P.; Malhotra, N.; Lai, Y.-H.; Liang, S.-T.; Chen, J.-R.; Chen, K.H.-C.; Hsiao, C.-D. Nanoplastics Cause Neurobehavioral Impairments, Reproductive and Oxidative Damages, and Biomarker Responses in Zebrafish: Throwing up Alarms of Wide Spread Health Risk of Exposure. *Int. J. Mol. Sci.* **2020**, *21*, 1410. https://doi.org/10.3390/ijms21041410.
90. Duarte-Costa, S.; Castro-Ferreira, R.; Neves, J.S.; Leite-Moreira, A.F. S100A1: A Major Player in Cardiovascular Performance. *Physiol. Res.* **2014**, *63*, 669–681. https://doi.org/10.33549/physiolres.932712.
91. Kraemer, A.M.; Saraiva, L.R.; Korsching, S. Structural and functional diversification in the teleost S100 family of calcium-binding proteins. *BMC Evol. Biol.* **2008**, *8*, 48. https://doi.org/10.1186/1471-2148-8-48.
92. Thanassoulas, A.; Theodoridou, M.; Barrak, L.; Riguene, E.; Alyaarabi, T.; Elrayess, M.A.; Lai, F.A.; Nomikos, M. Arrhythmia-Associated Calmodulin E105A Mutation Alters the Binding Affinity of CaM to a Ryanodine Receptor 2 CaM-Binding Pocket. *Int. J. Mol. Sci.* **2023**, *24*, 15630. https://doi.org/10.3390/ijms242115630.
93. Pan, Y.K.; Ern, R.; Morrison, P.R.; Brauner, C.J.; Esbaugh, A.J. Acclimation to prolonged hypoxia alters hemoglobin isoform expression and increases hemoglobin oxygen affinity and aerobic performance in a marine fish. *Sci. Rep.* **2017**, *7*, 7834. https://doi.org/10.1038/s41598-017-07696-6.
94. Roesner, A.; Hankeln, T.; Burmester, T. Hypoxia induces a complex response of globin expression in zebrafish (*Danio rerio*). *J. Exp. Biol.* **2006**, *209*, 2129–2137. https://doi.org/10.1242/jeb.02243.
95. Pelster, B.; Egg, M. Hypoxia-inducible transcription factors in fish: Expression, function and interconnection with the circadian clock. *J. Exp. Biol.* **2018**, *221*, jeb163709. https://doi.org/10.1242/jeb.163709.
96. Merx, M.W.; Flögel, U.; Stumpe, T.; Gödecke, A.; Decking, U.K.M.; Schrader, J. Myoglobin facilitates oxygen diffusion. *FASEB J.* **2001**, *15*, 1077–1079. https://doi.org/10.1096/fsb2fj000497fje.
97. Hendgen-Cotta, U.B.; Esfeld, S.; Coman, C.; Ahrends, R.; Klein-Hitpass, L.; Flögel, U.; Rassaf, T.; Totzeck, M. A novel physiological role for cardiac myoglobin in lipid metabolism. *Sci. Rep.* **2017**, *7*, 43219. https://doi.org/10.1038/srep43219.
98. Elkholi, I.E.; Elsherbiny, M.E.; Emara, M. Myoglobin: From physiological roles to potential implications in cancer. *Biochim. Biophys. Acta (BBA)—Rev. Cancer* **2022**, *1877*, 188706. https://doi.org/10.1016/j.bbcan.2022.188706.
99. Schlosser, A.; Helfenrath, K.; Wisniewsky, M.; Hinrichs, K.; Burmester, T.; Fabrizius, A. The knockout of cytoglobin 1 in zebrafish (*Danio rerio*) alters lipid metabolism, iron homeostasis and oxidative stress response. *Biochim. Biophys. Acta (BBA)—Mol. Cell Res.* **2023**, *1870*, 119558. https://doi.org/10.1016/j.bbamcr.2023.119558.
100. Keen, A.N.; Fenna, A.J.; McConnell, J.C.; Sherratt, M.J.; Gardner, P.; Shiels, H.A. Macro- and micromechanical remodelling in the fish atrium is associated with regulation of collagen 1 alpha 3 chain expression. *Pflug. Arch. Eur. J. Physiol.* **2018**, *470*, 1205–1219. https://doi.org/10.1007/s00424-018-2140-1.
101. Emam, M.; Caballero-Solares, A.; Xue, X.; Umasuthan, N.; Milligan, B.; Taylor, R.G.; Balder, R.; Rise, M.L. Gill and Liver Transcript Expression Changes Associated With Gill Damage in Atlantic Salmon (*Salmo salar*). *Front. Immunol.* **2022**, *13*, 806484. https://doi.org/10.3389/fimmu.2022.806484.

102. Fraser, J.; de Mello, L.V.; Ward, D.; Rees, H.H.; Williams, D.R.; Fang, Y.; Brass, A.; Gracey, A.Y.; Cossins, A.R. Hypoxia-inducible myoglobin expression in nonmuscle tissues. *Proc. Natl. Acad. Sci. USA* **2006**, *103*, 2977–2981. https://doi.org/10.1073/pnas.0508270103.
103. Mairbäurl, H.; Weber, R.E. Oxygen Transport by Hemoglobin. *Compr. Physiol.* **2012**, *2*, 1463–1489. https://doi.org/10.1002/j.2040-4603.2012.tb00415.x.
104. Reeder, B.J. Redox and Peroxidase Activities of the Hemoglobin Superfamily: Relevance to Health and Disease. *Antioxidants Redox Signal.* **2017**, *26*, 763–776. https://doi.org/10.1089/ars.2016.6803.
105. Fago, A. Functional roles of globin proteins in hypoxia-tolerant ectothermic vertebrates. *J. Appl. Physiol.* **2017**, *123*, 926–934. https://doi.org/10.1152/japplphysiol.00104.2017.
106. Widmer, C.C.; Pereira, C.P.; Gehrig, P.; Vallelian, F.; Schoedon, G.; Buehler, P.W.; Schaer, D.J. Hemoglobin Can Attenuate Hydrogen Peroxide–Induced Oxidative Stress by Acting as an Antioxidative Peroxidase. *Antioxid. Redox Signal.* **2010**, *12*, 185–198. https://doi.org/10.1089/ars.2009.2826.
107. Li, D.; Chen, X.Q.; Li, W.-J.; Yang, Y.-H.; Wang, J.-Z.; Yu, A.C.H. Cytoglobin Up-regulated by Hydrogen Peroxide Plays a Protective Role in Oxidative Stress. *Neurochem. Res.* **2007**, *32*, 1375–1380. https://doi.org/10.1007/s11064-007-9317-x.
108. Zaman, M.; Khan, F.U.; Younas, W.; Noorullah, M.; Ullah, I.; Li, L.; Zuberi, A.; Wang, Y. Physiological and histopathological effects of polystyrene nanoparticles on the filter-feeding fish *Hypophthalmichthys molitrix*. *Sci. Total. Environ.* **2024**, *912*, 169376. https://doi.org/10.1016/j.scitotenv.2023.169376.
109. Yang, H.; Wang, Q.; Xi, Y.; Yu, W.; Xie, D.; Morisaki, H.; Morisaki, T.; Cheng, J. AMPD2 plays important roles in regulating hepatic glucose and lipid metabolism. *Mol. Cell. Endocrinol.* **2023**, *577*, 112039. https://doi.org/10.1016/j.mce.2023.112039.
110. Pramfalk, C.; Ahmed, O.; Pedrelli, M.; Minniti, M.E.; Luquet, S.; Denis, R.G.; Olin, M.; Härdfeldt, J.; Vedin, L.; Steffensen, K.R.; et al. *Soat2* ties cholesterol metabolism to β-oxidation and glucose tolerance in male mice. *J. Intern. Med.* **2022**, *292*, 296–307. https://doi.org/10.1111/joim.13450.
111. Da Dalt, L.; Pedrelli, M.; Pramfalk, C.; Norata, G.; Parini, P. Cholesterol trapping by SOAT1 induces mitochondrial cholesterol accumulation and decrease oxidative metabolism. *Atherosclerosis* **2022**, *355*, 86. https://doi.org/10.1016/j.atherosclerosis.2022.06.486.
112. Ge, Y.; Yang, S.; Zhang, T.; Gong, S.; Wan, X.; Zhu, Y.; Fang, Y.; Hu, C.; Yang, F.; Yin, L.; et al. Ferroptosis participated in inhaled polystyrene nanoplastics-induced liver injury and fibrosis. *Sci. Total. Environ.* **2024**, *916*, 170342. https://doi.org/10.1016/j.scitotenv.2024.170342.
113. Bonnans, C.; Chou, J.; Werb, Z. Remodelling the extracellular matrix in development and disease. *Nat. Rev. Mol. Cell Biol.* **2014**, *15*, 786–801. https://doi.org/10.1038/nrm3904.
114. Martín, J.; Santos, J.L.; Aparicio, I.; Alonso, E. Microplastics and associated emerging contaminants in the environment: Analysis, sorption mechanisms and effects of co-exposure. *Trends Environ. Anal. Chem.* **2022**, *35*, e00170. https://doi.org/10.1016/j.teac.2022.e00170.
115. 118. de la Serrana, D.G.; Mareco, E.A.; LA Vieira, V.; Power, D.M.; Johnston, I.A. Comparison of the transcriptional responses of skeletal muscle and bone to a flooding dose of leucine in the gilthead sea bream (*Sparus aurata*). *Comp. Biochem. Physiol. Part B Biochem. Mol. Biol.* **2016**, *199*, 50–57. https://doi.org/10.1016/j.cbpb.2016.02.003.
116. Wistow, G.; Wyatt, K.; David, L.; Gao, C.; Bateman, O.; Bernstein, S.; Tomarev, S.; Segovia, L.; Slingsby, C.; Vihtelic, T. γN-crystallin and the evolution of the βγ-crystallin superfamily in vertebrates. *FEBS J.* **2005**, *272*, 2276–2291. https://doi.org/10.1111/j.1742-4658.2005.04655.x.
117. Lin, J.; Pan, D.; Zhu, Y.; Shen, B.; Sun, Z.; Zheng, Y.; Yin, Y.; Huang, C.; Wu, W.; Song, Y.; et al. Polystyrene nanoplastics chronic exposure cause zebrafish visual neurobehavior toxicity through TGFβ-crystallin axis. *J. Hazard. Mater.* **2025**, *492*, 138255. https://doi.org/10.1016/j.jhazmat.2025.138255.
118. Horwitz, J. Alpha-crystallin. *Exp. Eye Res.* **2003**, *76*, 145–153. https://doi.org/10.1016/s0014-4835(02)00278-6.
119. Rao, P.; Horwitz, J.; Zigler, J. α-Crystallin, a Molecular Chaperone, Forms a Stable Complex with Carbonic Anhydrase upon Heat Denaturation. *Biochem. Biophys. Res. Commun.* **1993**, *190*, 786–793. https://doi.org/10.1006/bbrc.1993.1118.
120. Kumar, P.A.; Reddy, G.B. Modulation of α-crystallin chaperone activity: A target to prevent or delay cataract? *IUBMB Life* **2009**, *61*, 485–495. https://doi.org/10.1002/iub.176.
121. Slingsby, C.; Wistow, G.J.; Clark, A.R. Evolution of crystallins for a role in the vertebrate eye lens. *Protein Sci.* **2013**, *22*, 367–380. https://doi.org/10.1002/pro.2229.

122. Ramírez-Rodríguez, G.; Babu, H.; Klempin, F.; Krylyshkina, O.; Baekelandt, V.; Gijsbers, R.; Debyser, Z.; Overall, R.W.; Nicola, Z.; Fabel, K.; et al. The α Crystallin Domain of Small Heat Shock Protein b8 (Hspb8) Acts as Survival and Differentiation Factor in Adult Hippocampal Neurogenesis. *J. Neurosci.* **2013**, *33*, 5785–5796. https://doi.org/10.1523/jneurosci.6452-11.2013.
123. Coop, A.; Wiesmann, K.E.; Crabbe, M.C. Translocation of β crystallin in neural cells in response to stress. *FEBS Lett.* **1998**, *431*, 319–321. https://doi.org/10.1016/s0014-5793(98)00783-2.
124. Marvin, M.; O'Rourke, D.; Kurihara, T.; Juliano, C.E.; Harrison, K.L.; Hutson, L.D. Developmental expression patterns of the zebrafish small heat shock proteins. *Dev. Dyn.* **2008**, *237*, 454–463. https://doi.org/10.1002/dvdy.21414.
125. Park, J.; MacGavin, S.; Niederbrach, L.; Mchaourab, H.S. Interplay between Nrf2 and αB-crystallin in the lens and heart of zebrafish under proteostatic stress. *Front. Mol. Biosci.* **2023**, *10*, 1185704. https://doi.org/10.3389/fmolb.2023.1185704.
126. Zhang, Y.; Wang, Z.; Zhao, G.; Liu, J.-X. Silver nanoparticles affect lens rather than retina development in zebrafish embryos. *Ecotoxicol. Environ. Saf.* **2018**, *163*, 279–288. https://doi.org/10.1016/j.ecoenv.2018.07.079.
127. Shin, J.-H.; Kim, S.-W.; Lim, C.-M.; Jeong, J.-Y.; Piao, C.-S.; Lee, J.-K. αB-crystallin suppresses oxidative stress-induced astrocyte apoptosis by inhibiting caspase-3 activation. *Neurosci. Res.* **2009**, *64*, 355–361. https://doi.org/10.1016/j.neures.2009.04.006.
128. Chis, R.; Sharma, P.; Bousette, N.; Miyake, T.; Wilson, A.; Backx, P.H.; Gramolini, A.O. α-Crystallin B prevents apoptosis after H_2O_2 exposure in mouse neonatal cardiomyocytes. *Am. J. Physiol. Circ. Physiol.* **2012**, *303*, H967–H978. https://doi.org/10.1152/ajpheart.00040.2012.
129. Thorkelsson, A.; Chin, M.T. Role of the Alpha-B-Crystallin Protein in Cardiomyopathic Disease. *Int. J. Mol. Sci.* **2024**, *25*, 2826. https://doi.org/10.3390/ijms25052826.
130. Smith, A.A.; Wyatt, K.; Vacha, J.; Vihtelic, T.S.; Zigler, J.S.; Wistow, G.J.; Posner, M. Gene duplication and separation of functions in αB-crystallin from zebrafish (*Danio rerio*). *FEBS J.* **2006**, *273*, 481–490. https://doi.org/10.1111/j.1742-4658.2005.05080.x.
131. Blaner, W.S. Retinol-Binding Protein: The Serum Transport Protein for Vitamin A*. *Endocr. Rev.* **1989**, *10*, 308–316. https://doi.org/10.1210/edrv-10-3-308.
132. Kaushik, V.; Gessa, L.; Kumar, N.; Fernandes, H. Towards a New Biomarker for Diabetic Retinopathy: Exploring RBP3 Structure and Retinoids Binding for Functional Imaging of Eyes In Vivo. *Int. J. Mol. Sci.* **2023**, *24*, 4408. https://doi.org/10.3390/ijms24054408.
133. Nickerson, J.M.; Frey, R.; Ciavatta, V.T.; Stenkamp, D.L. Interphotoreceptor retinoid-binding protein gene structure in tetrapods and teleost fish. *Mol. Vis.* **2006**, *12*, 1565–1585.
134. Liou, G.I.; Fei, Y.; Peachey, N.S.; Matragoon, S.; Wei, S.; Blaner, W.S.; Wang, Y.; Liu, C.; Gottesman, M.E.; Ripps, H. Early Onset Photoreceptor Abnormalities Induced by Targeted Disruption of the Interphotoreceptor Retinoid-Binding Protein Gene. *J. Neurosci.* **1998**, *18*, 4511–4520. https://doi.org/10.1523/jneurosci.18-12-04511.1998.
135. Zeng, S.; Zhang, T.; Madigan, M.C.; Fernando, N.; Aggio-Bruce, R.; Zhou, F.; Pierce, M.; Chen, Y.; Huang, L.; Natoli, R.; et al. Interphotoreceptor Retinoid-Binding Protein (IRBP) in Retinal Health and Disease. *Front. Cell. Neurosci.* **2020**, *14*, 577935. https://doi.org/10.3389/fncel.2020.577935.
136. Gonzalez-Fernandez, F.; Sung, D.; Haswell, K.M.; Tsin, A.; Ghosh, D. Thiol-dependent antioxidant activity of interphotoreceptor retinoid-binding protein. *Exp. Eye Res.* **2014**, *120*, 167–174. https://doi.org/10.1016/j.exer.2014.01.002.
137. Gonzalez-Fernandez, F.; Betts-Obregon, B.; Yust, B.; Mimun, J.; Sung, D.; Sardar, D.; Tsin, A.T. Interphotoreceptor Retinoid-Binding Protein Protects Retinoids from Photodegradation. *Photochem. Photobiol.* **2015**, *91*, 371–378. https://doi.org/10.1111/php.12416.
138. Shao, C.; Bao, B.; Xie, Z.; Chen, X.; Li, B.; Jia, X.; Yao, Q.; Ortí, G.; Li, W.; Li, X.; et al. The genome and transcriptome of Japanese flounder provide insights into flatfish asymmetry. *Nat. Genet.* **2017**, *49*, 119–124. https://doi.org/10.1038/ng.3732.
139. Laudet, V.; Ravasi, T. *Evolution, Development and Ecology of Anemonefishes*, 1st ed.; CRC Press: Boca Raton, FL, USA, 2022.
140. de Jong, W.W.; Caspers, G.-J.; Leunissen, J.A. Genealogy of the α-crystallin—Small heat-shock protein superfamily. *Int. J. Biol. Macromol.* **1998**, *22*, 151–162. https://doi.org/10.1016/s0141-8130(98)00013-0.
141. Sendra, M.; Pereiro, P.; Yeste, M.; Mercado, L.; Figueras, A.; Novoa, B. Size matters: Zebrafish (*Danio rerio*) as a model to study toxicity of nanoplastics from cells to the whole organism. *Environ. Pollut.* **2021**, *268*, 115769. https://doi.org/10.1016/j.envpol.2020.115769.
142. Chisada, S.; Yoshida, M.; Karita, K. Ingestion of polyethylene microbeads affects the growth and reproduction of medaka, *Oryzias latipes*. *Environ. Pollut.* **2019**, *254*, 113094. https://doi.org/10.1016/j.envpol.2019.113094.
143. Yu, F.; Jin, F.; Cong, Y.; Lou, Y.; Li, Z.; Li, R.; Ding, B.; Wang, Y.; Chen, J.; Wang, J. Bisphenol A decreases the developmental toxicity and histopathological alterations caused by polystyrene nanoplastics in developing marine medaka *Oryzias melastigma*. *Chemosphere* **2023**, *336*, 139174. https://doi.org/10.1016/j.chemosphere.2023.139174.

144. Winston, G.W.; Regoli, F.; Dugas, A.J.; Fong, J.H.; Blanchard, K.A. A Rapid Gas Chromatographic Assay for Determining Oxyradical Scavenging Capacity of Antioxidants and Biological Fluids. *Free. Radic. Biol. Med.* **1998**, *24*, 480–493, https://doi.org/10.1016/s0891-5849(97)00277-3.
145. Regoli, F.; Winston, G.W. Quantification of Total Oxidant Scavenging Capacity of Antioxidants for Peroxynitrite, Peroxyl Radicals, and Hydroxyl Radicals. *Toxicol. Appl. Pharmacol.* **1999**, *156*, 96–105, https://doi.org/10.1006/taap.1999.8637.
146. Lowry, O.H.; Rosebrough, N.J.; Farr, A.L.; Randall, R.J. Protein measurement with the Folin phenol reagent. *J. Biol. Chem.* **1951**, *193*, 265–275. https://doi.org/10.1016/s0021-9258(19)52451-6.